2014-09

Feasibility of single and dual satellite systems to enable continuous communication capability to a manned Mars mission

Gladem, Jennifer

Monterey, California: Naval Postgraduate School

NAVAL POSTGRADUATE SCHOOL

MONTEREY, CALIFORNIA

THESIS

FEASIBILITY OF SINGLE AND DUAL SATELLITE SYSTEMS TO ENABLE CONTINUOUS COMMUNICATION CAPABILITY TO A MANNED MARS MISSION

by

Jennifer Gladem

September 2014

Thesis Advisor: Daniel Bursch
Second Reader: Brian Steckler

Approved for public release; distribution is unlimited

THIS PAGE INTENTIONALLY LEFT BLANK

REPORT DOCUMENTATION PAGE

Form Approved OMB No. 0704-0188

1. AGENCY USE ONLY *(Leave blank)*	**2. REPORT DATE** September 2014	**3. REPORT TYPE AND DATES COVERED** Master's Thesis

4. TITLE AND SUBTITLE
FEASIBILITY OF SINGLE AND DUAL SATELLITE SYSTEMS TO ENABLE CONTINUOUS COMMUNICATION CAPABILITY TO A MANNED MARS MISSION

5. FUNDING NUMBERS

6. AUTHOR(S) Jennifer Gladem

7. PERFORMING ORGANIZATION NAME(S) AND ADDRESS(ES)
Naval Postgraduate School
Monterey, CA 93943-5000

8. PERFORMING ORGANIZATION REPORT NUMBER

9. SPONSORING /MONITORING AGENCY NAME(S) AND ADDRESS(ES)
N/A

10. SPONSORING/MONITORING AGENCY REPORT NUMBER

11. SUPPLEMENTARY NOTES The views expressed in this thesis are those of the author and do not reflect the official policy or position of the Department of Defense or the U.S. Government. IRB protocol number ____N/A____.

12a. DISTRIBUTION / AVAILABILITY STATEMENT
Approved for public release; distribution is unlimited

12b. DISTRIBUTION CODE
A

13. ABSTRACT (maximum 200 words)

The National Aeronautics and Space Administration's current proposed timeline for an interplanetary expedition is circa 2030. A manned Mars mission involves many complex requirements for communication with significant challenges including implementation, signal limitations, orbit requirements, and Earth-Sun-Mars occlusion.

This analysis is focused on the potential advantages and disadvantages of potential orbits for maintaining communications with a manned mars mission. Areas analyzed will include signal limitations and possible improvements for Mars communication, through recommended frequency, the resulting signal to noise ratio, available channel capacity, and possible data rates of potential orbits.

Ultimately, the purpose of this study is to determine (1) will one to two satellites be capable of maintaining continuous communication between a Mars orbit and a Mars ground mission, (2) will one to two satellites be capable of maintaining communication between Mars and Earth, likely through the Deep Space Network (DSN), (3) which frequency or frequencies will best suit Earth-Mars, and Mars relay communication, (4) how many satellites are necessary for continuous communication, including during Mars transit through the solar occlusion zone, and (5) what orbits are necessary to provide continuous communications throughout all the above mission regimes?

14. SUBJECT TERMS
Mars, satellite communication, Deep Space Network (DSN), Mars ground mission, manned Mars mission, Earth-Sun-Mars occlusion, signal limitations, orbital requirements

15. NUMBER OF PAGES
91

16. PRICE CODE

17. SECURITY CLASSIFICATION OF REPORT	**18. SECURITY CLASSIFICATION OF THIS PAGE**	**19. SECURITY CLASSIFICATION OF ABSTRACT**	**20. LIMITATION OF ABSTRACT**
Unclassified	Unclassified	Unclassified	UU

NSN 7540-01-280-5500

Standard Form 298 (Rev. 2-89)
Prescribed by ANSI Std. 239-18

THIS PAGE INTENTIONALLY LEFT BLANK

Approved for public release; distribution is unlimited

FEASIBILITY OF SINGLE AND DUAL SATELLITE SYSTEMS TO ENABLE CONTINUOUS COMMUNICATION CAPABILITY TO A MANNED MARS MISSION

Jennifer Gladem
Captain, United States Marine Corps
B.S., United States Naval Academy, 2003

Submitted in partial fulfillment of the
requirements for the degree of

MASTER OF SCIENCE IN INFORMATION TECHNOLOGY MANAGEMENT

from the

NAVAL POSTGRADUATE SCHOOL
September 2014

Author: Jennifer Gladem

Approved by: Daniel Bursch
Thesis Advisor

Brian Steckler
Second Reader

Dan C. Boger
Chair, Department of Information Sciences

THIS PAGE INTENTIONALLY LEFT BLANK

ABSTRACT

The National Aeronautics and Space Administration's current proposed timeline for an interplanetary expedition is circa 2030. A manned Mars mission involves many complex requirements for communication with significant challenges including implementation, signal limitations, orbit requirements, and Earth-Sun-Mars occlusion.

This analysis is focused on the potential advantages and disadvantages of potential orbits for maintaining communications with a manned mars mission. Areas analyzed will include signal limitations and possible improvements for Mars communication, through recommended frequency, the resulting signal to noise ratio, available channel capacity, and possible data rates of potential orbits.

Ultimately, the purpose of this study is to determine (1) will one to two satellites be capable of maintaining continuous communication between a Mars orbit and a Mars ground mission, (2) will one to two satellites be capable of maintaining communication between Mars and Earth, likely through the Deep Space Network (DSN), (3) which frequency or frequencies will best suit Earth-Mars, and Mars relay communication, (4) how many satellites are necessary for continuous communication, including during Mars transit through the solar occlusion zone, and (5) what orbits are necessary to provide continuous communications throughout all the above mission regimes?

THIS PAGE INTENTIONALLY LEFT BLANK

TABLE OF CONTENTS

LIST OF FIGURES

THIS PAGE INTENTIONALLY LEFT BLANK

LIST OF TABLES

THIS PAGE INTENTIONALLY LEFT BLANK

LIST OF ACRONYMS AND ABBREVIATIONS

AEP	artificial equilibrium point
BER	bit error Rate
CME	coronal mass ejection
DSN	Deep Space Network
EM	electromagnetic
LASCO	Large Angle and Spectrometric Coronagraph
MARSIS	Mars Advanced Radar for Subsurface and Ionospheric Sounding
MLT	Mars Lasercom Terminal
NASA	National Aeronautics and Space Administration
S/N	signal to noise ratio
SEP	solar electric propulsion
SOHO	Solar and Heliospheric Observatory
UHF	ultra high frequency

THIS PAGE INTENTIONALLY LEFT BLANK

ACKNOWLEDGMENTS

To my professors, instructors, mentors, and fellow students, thank you. Your patience, guidance, and gracious help have been invaluable to me and I cannot express my gratitude. To Joe, who fed me, put up with me, and did his best to assuage the vicious stress monster I became; to my family; and most of all to Sammy, whose love and happy wagging tail made every day better.

THIS PAGE INTENTIONALLY LEFT BLANK

I. INTRODUCTION

As propagating waves, electromagnetic transmissions (EM) are subject to path losses. These losses include free space loss, absorption loss, diffraction, multipath loss, terrain, and atmospheric loss. Free space loss is caused by the diffusion of signal power over an increasing area, essentially as the signal travels it expands in three dimensions, this expansion decreases the power per unit area of the signal. At the receiver, this power loss is proportional to the distance traveled. Absorption occurs as the signal travels through a non-transparent medium as the medium absorbs a part of the transmitted signal. Diffraction is caused by interfering objects in the line of transmission, as signals can reflect but not "bend" diffraction losses are increased by rounded objects. Multipath loss is caused by the signal taking multiple paths to the receiver and their subsequent in phase or out of phase re-combination. Terrain affects the signal through obstruction and attenuation, dependent on the frequency, composition can also affect signal strength. Atmospheric loss similarly causes loss through both refraction and reflection. The troposphere has an especially significant effect, evident by ultra high a (UHF) "bouncing."

A. ATMOSPHERE

An atmosphere is the layer or envelope of gases surrounding a planet (*Merriam Webster*, 2014). It is critical and largely causal to the morphology of a planet. Additionally, in the case of Earth, atmosphere is crucial to the evolution and survival of life.

1. Earth Atmosphere

Earth's atmosphere is comprised of roughly 78% nitrogen, 21% oxygen, 1% argon, and trace amounts of carbon dioxide, iodine, carbon monoxide, and ammonia with water vapor at low altitudes (Cain, 2009). This leads to significant attenuation by oxygen (which possesses a permanent magnetic moment) and attenuation by precipitation due to clouds. Water vapor attenuation is subject to many parameters, but is most affected

by droplet size, which can be represented by a logarithmic function of signal strength before, after, and through the rain region (Zubair, Haider, Khan, & Nasir, 2011).

2. Mars Atmosphere

In contrast, Mars' atmosphere is comprised of 96% carbon dioxide, 2.1% argon, 1.9% nitrogen, and traces of free oxygen, carbon monoxide, water, methane, nitrogen oxide, neon, hydrogen-deuterium-oxygen, krypton, and xenon (Mahaffy et al., 2013). This represents only 0.6% the volume of atmosphere surrounding Earth. However, Mars Exploration rovers indicated the Martian atmosphere is highly dusty as it contains a significant volume of suspended dust particles roughly 1.5 micrometers in diameter, which will affect high frequency signals.

B. ATMOSPHERIC EFFECTS

Based on the measurements from Viking 1, 2 and Mars 6, Seiff (1982) derived a nominal mean model of pressure and temperature shown below. This model was used by Ho, Golshan, and Kliore (2002) to tabulate the Martian tropospheric parameters and subsequently Martian tropospheric effects as functions of: temperature, pressure, and atmospheric mass density for a mid-latitude summer seasonal atmosphere where μ=43.49, R=191.18 joule/kg K, gravity g(z), and temperature T(z) are functions of altitude z

$$\frac{p}{p_0} = e - \frac{\mu}{R}\int_{z_0}^{z}\frac{g(z)}{T(z)}dz$$

Based on the Seiff (1982) model, in their paper, "Martian Atmospheric Effects on Radio Wave Propagation," Ho, Sue, and Golshan (2002) found the Martian atmospheric scale height (H_N) to be 11 km, which yields a refractive index (N) two orders of magnitude smaller than that of Earth, shown below where N_0 is the surface value of N (N_0=3.9N unit) when altitude h=0.

$$N(h) = N_0 * e^{(-\frac{h}{H_N})}$$

As such, ray bending and multipath loss are present but significantly lower than terrestrial losses. Due to the relative size of Mars (15% of Earth by volume, 11% of Earth

by mass) defocusing loss will be increased. Mars temperature fluctuations (120 K–293 K) are comparable to Earth (185 K–344.85 K) and when combined with the significantly thinner troposphere, Ho et al. (n.d.) indicate Mars scintillation losses represented in Figure 1 are likely less than 0.5% of Earth.

As shown by Ho et al. (n.d.), the thin atmosphere and low temperatures (average 210 K) also eliminate many Earth-like weather effects. Martian clouds have an average optical depth of 1.0 from 400–700 nm (visible range), equaling a 63.3% reduction of transiting signal. At their extreme, Martian clouds are similar to high-level cirrus clouds on Earth. Due to the relatively dry atmosphere (water content 1/3000th Earth) water absorption is low. Absorption losses are further decreased because the Martian atmosphere is predominately composed of CO_2 and N_2, which do not form electric or magnetic dipoles, though CO_2 and N_2 can through interaction at high density cause absorption lines in the infrared and visible bands. Ho Sue, and Golshan (2002) frequency versus attenuation is shown in Figure 1.

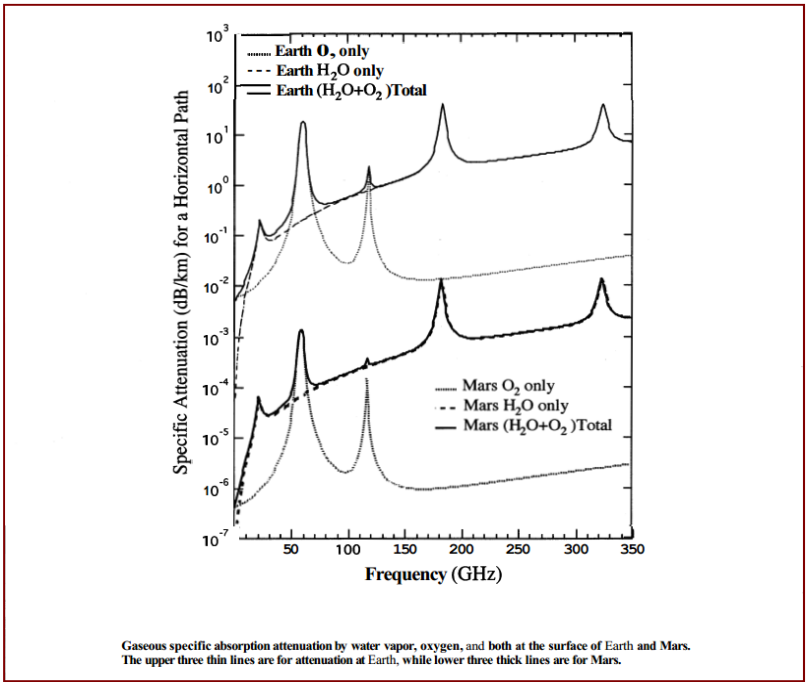

Figure 1. Gaseous specific absorption of Earth and Mars (from Ho, Sue, & Golshan, 2002)

Mars Advanced Radar for Subsurface and Ionospheric Sounding (MARSIS) data analyzed by Andrews et al. (2013) indicates a Martian plasma frequency range from 40 kHz to 231 kHz. Typical communications will not be affected however; during entry Mars Pathfinder experienced an expected 10 second plasma sheath blackout when plasma density surrounding the lander increased to over 8.8 x 10^{11} cm^{-3} (Ho, Sue, & Golshan, 2002).

1. Losses

Ho et al. (2002) calculates free space loss on Mars ranges from 277 dB to 294 dB between Mars and Earth. Earth tropospheric losses for Ka-band (26.5–40 GHz) average 3–4 dB but can be as great as 5 dB (vertical propagation) largely due to rain scattering and absorption. Mars tropospheric losses are dominated by dust storms, which average 1 dB but can be as large as 3 dB. Combined Martian atmospheric losses average from 1.4 to 2 dB but could be as great as 3.4 dB. Multipath losses can be extrapolated from Earth data and may be as high as 2–8 dB for L band signals, with higher losses expected at higher frequencies.

Ho et al. (2002) further calculated total expected Mars-Earth atmospheric losses will likely be near 8 dB. Simplified path loss between Mar-Earth can be calculated using

$$L_P = 20\log(\frac{4\pi D}{\lambda})$$

where D = maximum straight-line distance between Earth and Mars (this neglects the Sun occult region and equals 401E6 km), and λ = wavelength (34450 MHz uplink, 32050 MHz downlink), which yields a free space path loss of -295.2 dB uplink, and -294.6 downlink. Therefore, total losses are expected to be near 303 dB. To calculate losses incorporating a viable occult solution, additional, and potentially non-keplerian (B) orbits, must first be used.

2. Noise

The ITU Radiocommunication Assembly identifies sources of radio noise external to the radio receiving system for Earth-space communications as from the

following: atmospheric noise (including lightning), radiation from machinery and or transmission lines, emissions from atmospheric gases and hydrometeors, obstruction, and celestial sources. Noises from such sources are typically given in terms of brightness temperature.

External noise figures (dB) and sky temperatures (K) versus frequency calculated by Ho, Slobin, Sue, and Njoku (2002) in "Mars Background Noise Temperatures Received by Spacecraft Antennas" are given in Figure 2.

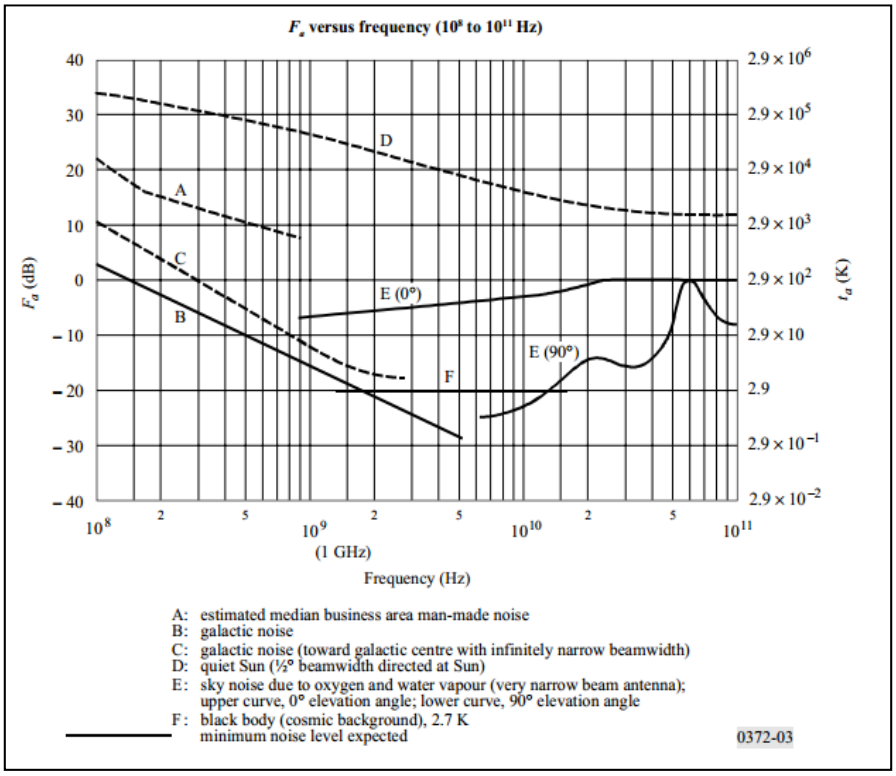

Figure 2. ITU-R P372-7 frequency vs. noise
(from ITU Radiocommunication Assembly, 2001)

Martian surface emissivity, a significant component of background noise, is dominated by surface temperature. Mars surface temperatures are lower than but comparable to Earth. Ho et al. (2002) calculate the antenna noise temperature for an antenna (pointing) at Mars and Earth (in degrees Kelvin). Ka-band is summarized in Table 1.

Table 1. Ka-band antenna temperature (K) at Mars and Earth (after Ho, Sue, & Golshan, 2002).

Downward Looking	Mars	193
	Earth	210
Upward Looking	Mars	3
	Earth	117

Using the Ho, Sue, and Golshan (2002) antenna noise temperatures, and an estimated Mars sky noise temperature of 5 K and an Earth average sky noise of 43 K (Ho, Slobin, & Gritton, 2005), total Ka-band receiver noise can be estimated using:

$$T = T_{ant} + T_{sys}$$

$$NF = 1 + \frac{T}{T_0}$$

$$N = kBT$$

Resultant Mars noise is shown in Table 2.

Table 2. Signal noise

	T_{ant} (K)		T (K)	NF	N (W)	N (dB)
Downward Looking	Mars	193	198	1.68	1.37E-12	-118
	Earth	210	253	1.87	1.75E-12	-117
Upward Looking	Mars	3	78	1.27	5.38E-13	-122
	Earth	117	166	1.57	1.15E-12	-119

where T_0 = 290 K, k = Boltzman's constant 1.3806488 x 10^{-23} noise temperature 5 K in Ka-band, downward looking is same as earth, surface mars 210K, 300K earth.

3. Gain

Antenna gain relates the intensity of an antenna in a given direction to that of a hypothetical lossless ideal antenna radiating equally in all directions. Using their gaseous attenuation model and a hypothetical 1 m dish antenna, Ho, Sue, and Golshan (2002) calculated background noise effects on the gain of a Mars based signal/receiver, across multiple bands as follows in Table 3.

Table 3. Antenna maximum and minimum gains by frequency (after Ho, Sue, & Golshan, 2002)

Band	UHF	S	X	Ka	Omni-directional
f (GHz)	0.4	2.3	8.4	32	
G_{max} (dB)	12	25.4	36	47	3
G_{min} (dB)	-3.6	-7.4	-10.2	-13	-1

This shows a clear gain advantage of high frequency Ka-band communications from and to Mars.

Current commercial Ka-band receiver antenna sizes range from 0.35 to 25m ("KA-band," n.d.). Assuming an efficiency of .7 and the Ka-band standards for transmission, the expected gain of a 0.3 m receiver antenna at the low limit of Ka-band is over 18 dB (SatCom Online, 2014).

Using antenna gain calculated from the standard antenna gain equation shown below, NASA's Deep Space Network (DSN) 70m antenna parameters include a Ka-band gain of over 85 dB and a maximum transmit power of 400 kW. The DSN 34m antenna posts a similarly impressive gain of 80 dB operating in the Ka-band. Additionally, NASA's recently developed inflatable/self-rigidizable antenna dish could provide similar efficiency with a 24 m^2 area and subsequent 63 dB of gain

$$G = 10\log(\frac{4\pi A_r \eta}{\lambda^2})$$

where A_r = physical aperture area, λ= wavelength in meters at the frequency of operation (34450 MHz uplink 32050 MHz downlink), and η = aperture efficiency (70%).

C. LINK BUDGET

Therefore, the downlink budget in dB of Mars communication can be expressed as

$$P_r = P_t + G_t + G_r - L_p$$

where P_r = power received, P_t = power transmitted, G_t = gain of the transmit antenna, G_r = gain of the receive antenna, and L_p – path loss, which = free space loss + atmospheric loss.

D. BASELINE ESTIMATES (NOT A VIABLE OCCLUSION SOLUTION)

Assuming a DSN transmission power of 400 kW (its maximum output), the signal received from Earth to Mars should be near -96.2 dB. A signal received from Mars (assuming an unrealistic orbiter transmission power of 400 kW) should be near -96.9 dB. Assuming a more realistic safety restricted DSN transmit power of 20 kW, and viable orbiter transmission power of 100 W, the received signals should be near -115 dB and -139 dB, respectively. transmission link budgets are summarized in Table 4.

Table 4. Baseline link budgets

	Transmit Power	**Gain Transmitter**	**Gain Receiver**	**Loss (Free space + atmospheric)**	**Received Power**
Uplink 70 m (34450MHz)	400kW=56.02dBW	86.5	64.4	295.2+8=303.2	-96.3
Downlink 70m (32050 MHz)	400kW=56.02dBW	63.8	85.9	294.6+8=302.6	-96.9
Uplink 34 m (34450 MHz)	400kW=56.02dBW	80.2	64.4	295.2+8=303.2	-102.6
Downlink 34 m (32050 MHz)	400kW=56.02dBW	63.8	79.6	294.6+8=302.6	-103.2
Uplink 70 m (34450MHz)	20kW=43 dBW	86.5	64.4	295.2+8=303.2	-109.3
Downlink (32050 MHz) Low Power	100W=20dBW	63.8	85.7	294.6+8=302.6	-132.93
Uplink 34 m (34450 MHz)	20kW=43 dBW	80.2	64.4	295.2+8=303.2	-115.6
Downlink (32050 MHz) Low Power	100W=20dBW	63.8	79.6	294.6+8=302.6	-139.2

E. SIGNAL TO NOISE RATIO

Signal to noise ratio (S/N or S/N) is a comparison of the desired signal power to the background noise. It is typically expressed in decibels where any positive value indicates a greater presence of signal than noise. Mathematically, it is expressed as:

$$\frac{S}{N} = \frac{P_{signal}}{P_{noise}}$$

or

$$\frac{S}{N} = 10\log_{10}(P_{signal}/P_{noise}) = P_{signal,dB} - P_{noise,dB}$$

The Shannon-Hartley theorem describes the channel capacity or maximum information rate based on the S/N. The channel capacity in bits per second is expressed as:

$$C = B\log_2 1 + \frac{S}{N}$$

where B equals the bandwidth in Hz, and S/N is a unit less ratio of W/W.

The E_b/N_0 or energy per bit to noise power spectral density ratio is used to compare bit error rate (BER) performance of different modulation schemes within digital communications. It is a normalized S/N or S/N per bit ("E_b/N_0," 2014). It can be expressed as:

$$\frac{E_B}{N_0} = \frac{S}{N} * \left(\frac{B}{C}\right)$$

The spectral efficiency in bits/Hz expresses the net bit rate or maximum throughput over the bandwidth of a communication channel. It is used to analyze the efficiency of digital modulation often in combination with forward error correction.

Ultimately based on averaged noise temperatures of Earth and Mars ("DSN Telecommunications," n.d.; Ho et al., 2002; Ho, Sue, & Golshan, 2002; Shambayati, et al., 2014; Taylor, Lee, & Shambayati, 2006), the best case (high power large dish uplink) S/N is 172.4 dB and worst case (medium dish low power downlink) S/N is 0.022 dB, which yield channel capacities of 3.72 Gbps, and 15.9 Mbps, and Eb/N0s of 23.2 and 0.701. An over 1000% increase from the Mars Reconnaissance Orbiter's average downlink speed on X-band (Taylor, Lee, & Shambayati, 2006).

THIS PAGE INTENTIONALLY LEFT BLANK

II. ORBITS AND INTRODUCTION TO NON-KEPLERIAN ORBITS

An orbit is the gravitationally curved path of an object around a point in space (barycenter), or alternately, the path followed by a celestial body or artificial satellite as it revolves around another body due to the force of gravity. In the case of a celestial body or satellite, the barycenter is the center of mass of the system. Orbits are elliptical or nearly circular in shape and are very closely approximated by Kepler's laws of planetary motion ("Orbit," n.d.).

Planetary motion within our own solar system was mapped and understood for its periodicity for many centuries but it was not until Johannes Kepler (1619), a German mathematician, developed his three laws of planetary motion in the early 17th century that the solar system was accurately modeled and more importantly, the movements of the planets successfully predicted.

A. KEPLERIAN ORBITS

Johannes Kepler was a brilliant mathematician hired to map the orbit of Mars by the infamous elk owner, duelist, and astronomer Tycho Brahe (Dreyer & Brahe, 1890). Despite a difference in viewpoints (Kepler supported Copernicus while Brahe developed his own model of planetary motion in which the Sun orbited the Earth and all other bodies orbited the Sun), Kepler eventually inherited Brahe's detailed astronomical records, and using Brahe's data, Kepler ultimately showed not only did the planets orbit the Sun, but the planets' orbits were elliptical with the Sun at one focus point (Kepler, 1622). Kepler (1619) further determined the planets traced a path of continuous area per unit time (they moved much faster when nearer the Sun), and ultimately, found the period is directly and mathematically related to the planet's distance from the Sun. These three ideas became Kepler's three laws of planetary motion illustrated in Figure 3.

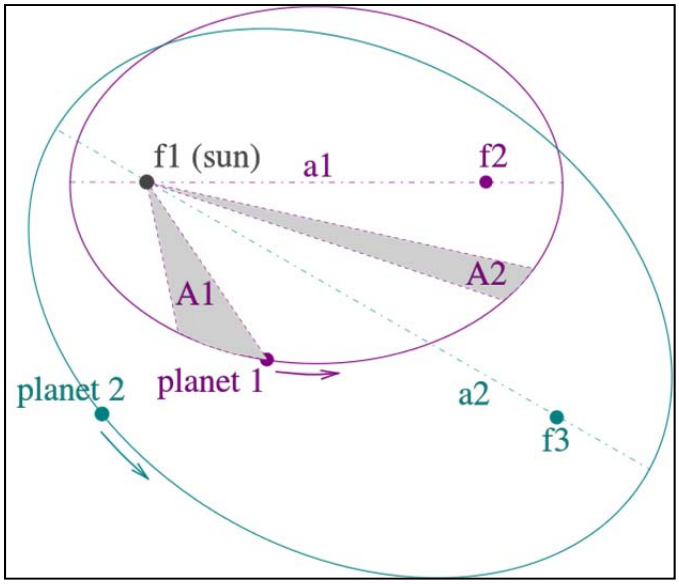

Figure 3. Kepler's laws (from Stundle, 2007)

In Figure 3, f1 and f2 depict the foci of the system of the Sun and two planets, a1 and a2 depict the semi-major axes, and A1 and A2 show area cross sections carved by equal orbit times.

Following Kepler's publication of his three laws, Isaac Newton proved Kepler's laws adhered to his, then new, concept of gravity. To illustrate gravity, Newton described the motions of an apple from a tree and the moon around the earth as adhering "To the same natural effects," and further stated, "we must as far as possible, assign the same causes" ("The Science," 2009). In his breakthrough work, *Philosophiae Naturalis Principia Mathematica*, Newton described his own three laws of motion, and more importantly, defined the concept of universal gravitation, which ultimately provided the mechanism for Earth's movement around the Sun, and consequently, provided a plausible basis of motion for Kepler's laws (*Newton*, 1687).

A Keplerian orbit as expressed by Lemmon and Mondragon (2010) is:

$$l^2 = GMa(1 - e^2)$$

where l = angular momentum per unit mass, G = the gravitational constant or 6.670E-11 $m^3kg^{-1}s^{-2}$, M = 1.989E30 kg (the mass of the Sun), a = the semi-major axis of the orbit, and e = orbit eccentricity.

The current model of the solar system is built on Albert Einstein's principle of relativity and supported by data from the 1970 Mariner Spacecraft, the 2003 Cassini spacecraft, as well as NASA's Gravity B probe ("Einstein's General Relativity," 1970; Perrotto, 2011; "Saturn-bound Spacecraft," 2003). The relativistic correction as defined by Tyler J. Lemmon and Antonio R. Mondragon (2010) in their paper "First-Order Relativistic Corrections to Kepler's Orbits" is:

$$\epsilon \approx \frac{GM}{c^2 a(1-e^2)}$$

and is greatest for planets close to the Sun or with very eccentric orbits (Lemmon & Mondragon, 2010).

In general, using special relativity accounts for one sixth of the observed planetary orbit discrepancy (roughly 43 arcsec/century) (Lemmon & Mondragon, 2010); therefore, modeling the solar system (and subsequent three body satellite problems) as a Keplerian orbit problem is sufficient for this communication capability analysis.

Keplerian orbits account for the rotation of the vast majority of celestial bodies within our solar system. Notable anomalies are the non-Keplerian propeller moons in orbit within Saturn's rings (Tiscareno et al., 2010). Keplerian orbits trace a path of an ellipse, parabola, or hyperbola (escape orbit) and belong to a group of curves known as conic sections. Their mathematic expression is:

$$r(v) = \frac{a(1-e^2)}{1+e\cos(v)}$$

where r = the distance, a = the semi major axis, e = the orbit eccentricity, and ν = the true anomaly (the angle between the orbiting body and its closest approach to the central body, periapsis).

Based on their eccentricity (e) Keplerian orbits can be geometrically illustrated, as shown in Figure 4.

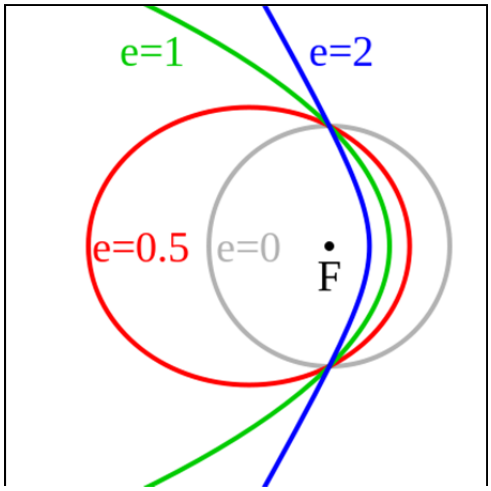

Figure 4. Keplerian orbits of various eccentricity (from Hill, n.d.)

Keplerian orbits are also identified as conic sections ("Conic Section," n.d), which describe an orbit as the intersection of a plane and a cone. Dependent upon the angle of intersection, the resulting curve takes the shape of a parabola, circle, ellipse, or a hyperbole, shown in Figures 5 and 6.

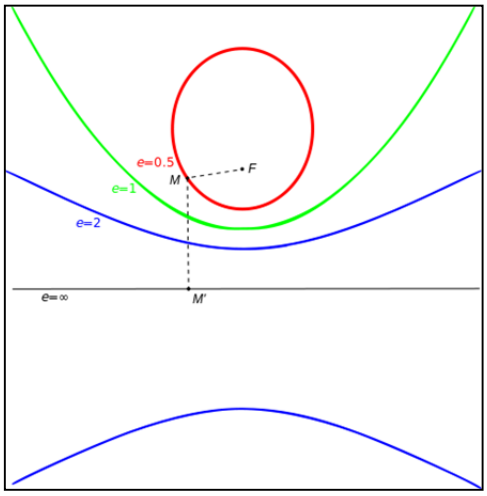

Figure 5. Conic sections (from Seahen, n.d.)

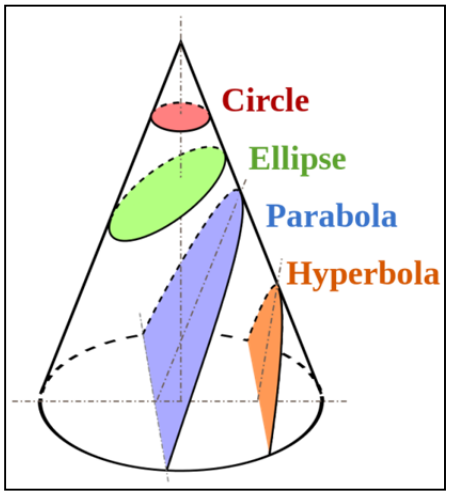

Figure 6. Conic sections (from S.A, n.d.)

In addition to describing planetary motion around the Sun, Keplerian orbits also describe satellite motion around a planet.

B. SATELLITE ORBITS

Satellite communications via a geosynchronous satellite were first suggested by Arthur C. Clarke in the October 1945 issue of *Wireless World* ("Clarke Suggests," 2013). Since then satellites have become an integral part of daily life. Over 6,600 satellites have been launched with an estimated 3,600 still in (Keplerian) orbit (Rising, 2013).

Satellites provide relays for communication across the globe and between spacecraft. They have enabled our present EM environment. However, as Keplerian orbiting bodies, satellites are restricted to a narrow field of stable orbits. These orbits limit the reach of satellite communications, which, in some cases, are completely unable to provide access. One such case is occultance where one body blocks an observer's view of another object by passing between them. A simple example of an occultance is a solar eclipse by the moon. In the case of a manned Mars mission, the greatest period of downed communications is caused by a solar occultance of the Earth-Mars system shown in Figure 7 (Provo, 2011b). This region occupies a roughly 5° arc as seen from Earth, which exceeds the diameter of the Sun significantly, but is still affected by solar interference (Provo, 2011a). In order to avoid this outage, Lagrange points or non-Keplerian orbits must be used.

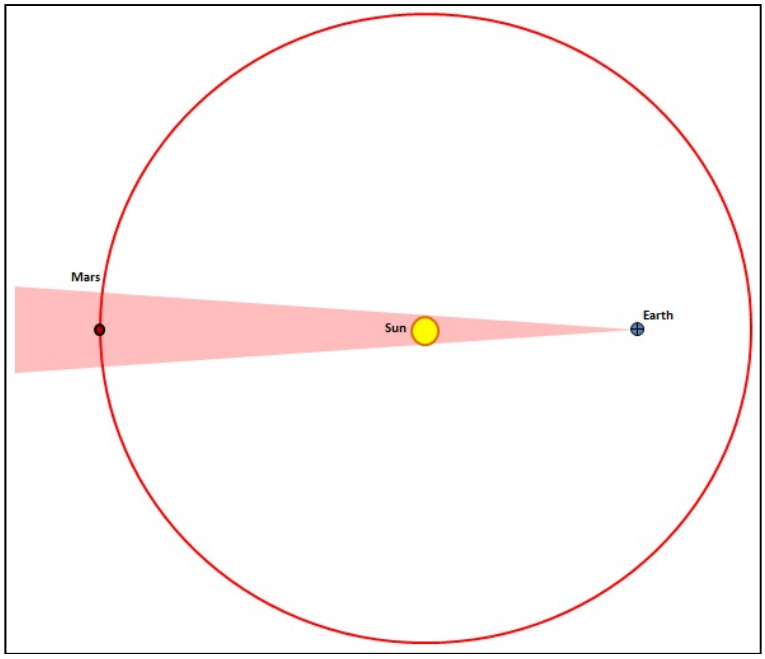

Figure 7. Earth-Sun-Mars occult region (from Provo, 2011b)

C. NON-KEPLERIAN ORBITS

Using the Keplerian model of the solar system, and the Earth-Sun-Mars 3-body system, Robert J. McKay, Malcolm Macdonald, James Biggs, Colin McInnes, and Massimiliano Vasile, in their papers, "Survey of Highly-Non-Keplerian Orbits with Low-Thrust Propulsion" (McKay, Macdonald, Biggs, & McInnes, 2011), and "Non-Keplerian Orbits using Low Thrust, High ISP Propulsion Systems" (McKay, Malcolm, Bosquilion de Frescheville, Vasile, McInnes & Biggs, 2009) describe a potential solution to communications blackouts caused by the Sun occult region.

To summarize McKay et al. the possibility of holding an object in artificial equilibrium through continuous application of low thrust propulsion against the difference in gravitation and centripetal force was first proposed by Dusek in 1966 (McKay et al., 2009). Since then, the potential for continuous low thrust propulsion has been expanded, allowing for the possibility of expanding a spacecraft's trajectory out of natural (Keplerian or A) orbits into displaced (non-Keplerian or B) orbits. These B orbits include the "orbit" of hovering above the pole of a planet as a "Statite" as described by Forward in the early 1990s (1991).

Alternately, McInnes (1998) described the conditions for circular displaced non-Keplerian orbits using an (x, y, z) reference frame and spacecraft of mass m rotating at constant angular velocity ω, shown in the following equations:

$$\ddot{r} + 2\omega \times \dot{r} + \nabla V = a$$

where r is the position vector with dots differentiated with respect to time, and V is the augmented potential (shown below)

$$V = -\left[\frac{1-\mu}{\|r_1\|} + \frac{\mu}{\|r_2\|}\right] + \frac{1}{2}\|\omega \times r\|^2$$

and a represents the applied thrust where n is the direction of thrust and G is the gravitational constant (equal to 1) making μ the reduced mass.

$$\mu = \frac{m_1}{m_1 + m_2}$$

$$a = [T/m]n$$

By setting $\ddot{r} = \dot{r} = 0$ (setting equilibrium conditions in the rotating frame) McInnes (1998) then simplified the equation to:

$$\nabla V = -a$$

which defines a surface of points at equilibrium, which subsequently, makes it possible to readily find and plot equilibrium points for a variety of forces (propulsion capabilities). The thrust vector for these points is given by

$$n = \frac{\nabla V}{\|\nabla V\|}$$

and the magnitude of the thrust vector is given by

$$\|a\| = \|\nabla V\|$$

Ultimately, the above equations allowed McInnis to treat the spacecraft as a stationary body within the reference frame, and then categorize two trajectories using continuous thrust. The first category is a displaced traditional (Keplerian orbit), such as the shift of a geostationary orbit (around the equatorial plane), to a hover orbit above the

pole of a planet. The second category is displaced orbits at the Lagrange points of a system. Lagrange point orbits are discussed further later.

Using a three-body problem to approximate a satellite orbiting a planet within the solar system, McKay et al. (2009) identifies a spacecraft of mass m within a rotating reference frame comprised of fix masses m_1 and m_2 with the x axis linking the primary masses, and the y axis denoting the axis of rotation. This in turn creates a spacecraft position vector of $r=(x,y,z)^T$ or alternately position vectors of r_1 and r_2, which describe the spacecraft position with respect to m_1 and m_2. In this case, $r_1=(x+\mu,y,z)^T$ and $r_2=((x-(1-\mu),y,z)^T$, all of which are shown in Figure 8.

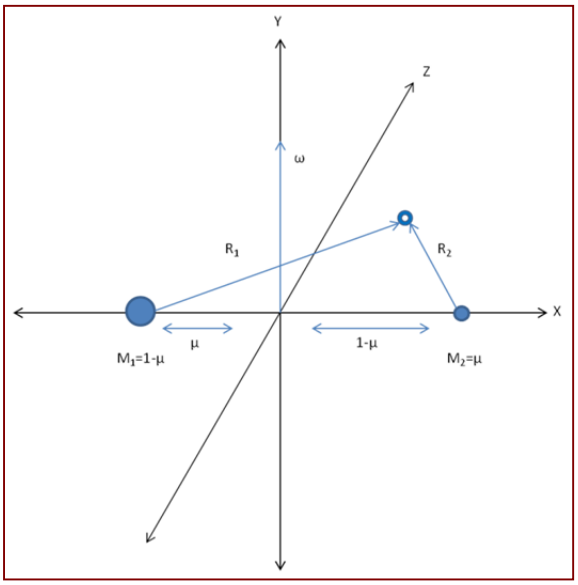

Figure 8. Rotating coordinate frame and spacecraft position for restricted three-body problem (after McKay et al., 2009)

At its limit, the three-body problem can be resolved as a two-body problem where the second mass m2=0, such as the case where the third body's mass is inconsequential in comparison to the much larger first and second bodies (i.e., a satellite in reference to a planet and the Sun). Using cylindrical polar coordinates (ρ ,z), and rotating with constant angular velocity $\omega = \omega\hat{z}$ relative to an inertial frame I, McKay et al. (2009) depicts the system in Figure 9.

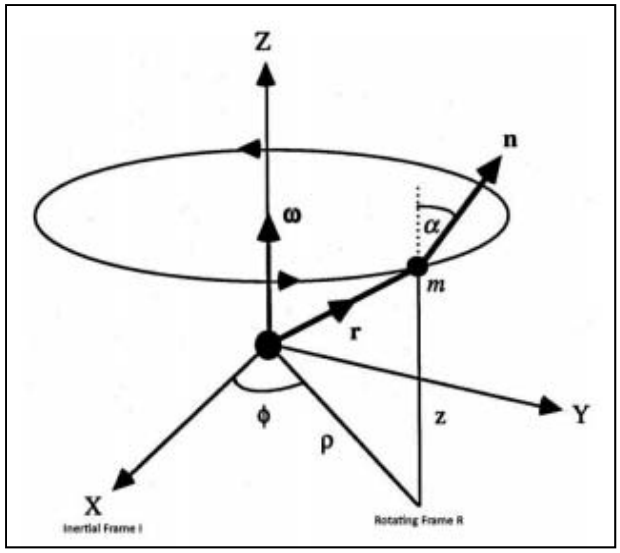

Figure 9. Two-body displaced non-Keplerian orbit (from McKay et al., 2009)

Because ω is constant, there is no transverse component of thrust. As such, the thrust vector exists solely in the plane of the radius vector and vertical axis, which consequently defines a single pitch angle, *a*, mathematically the system is:

$$V(\rho, z; \omega) = -[\tfrac{1}{2}(\rho\omega)^2 + \tfrac{GM}{r}]$$

$$\tan a = \frac{\|\hat{z} \times \nabla V\|}{\hat{z} \cdot \nabla V} = \left(\frac{\rho}{z}\right)\left[1 - \left(\frac{\omega}{\omega_0}\right)\right]^2$$

$$\omega_0 = \frac{GM}{r^3}$$

$$a(\rho, z; \omega) = [\rho^2(\omega^2 - \omega_0^2)^2 + z^2\omega_0^4]^{\frac{1}{2}}$$

all of which describes a stationary spacecraft within a rotating frame of reference or alternately within an inertial reference frame the spacecraft orbits in a displaced circle above the central body (a halo).

McKay et al. (2009) goes on to subdivide the first category of B orbits (halo orbits described above) into three types: Type I orbit period fixed for a given r, Type II orbit period fixed for a given ρ, and Type III Keplerian orbit (displaced orbit with the same orbital period as a selected Keplerian reference).

Type I orbits require the global minimum thrust, which makes the acceleration a function of ρ and z. Type II orbits describe a satellite that is synchronous with a body on a circular Keplerian orbit in the z=0 plane with a radius ρ. Type III orbits are synchronous with the Keplerian orbital period P, or the Keplerian orbital radius ρ.

McKay et al. (2009) Mars two and three-body B orbits are depicted in ρ –z contour plots, Figures 10–12. The dashed lines represent contours of constant period, the colored contours represent thrust contours (in mN), and the arrows show thrust direction required to maintain orbit. The thick black contour defines the limit of Mars (gravitational) influence.

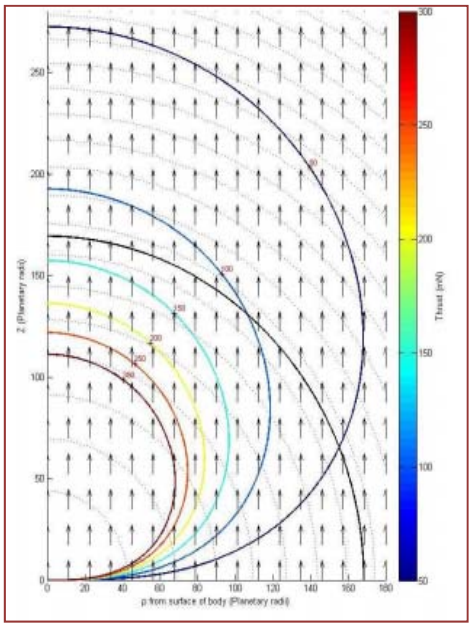

Figure 10. Mars two-body type I orbits (from McKay et al, 2011)

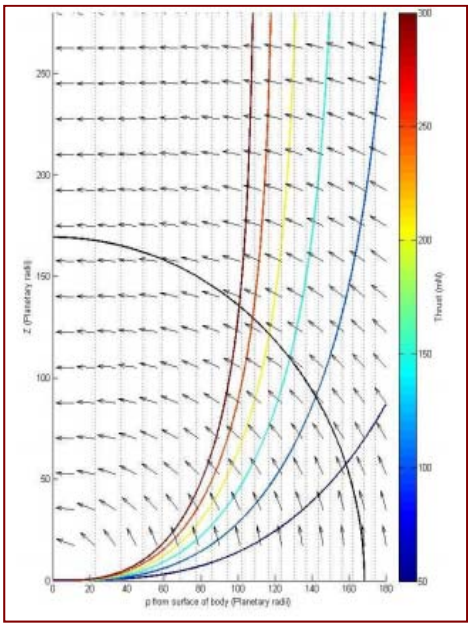

Figure 11. Mars two-body type II orbits (from McKay et al., 2011)

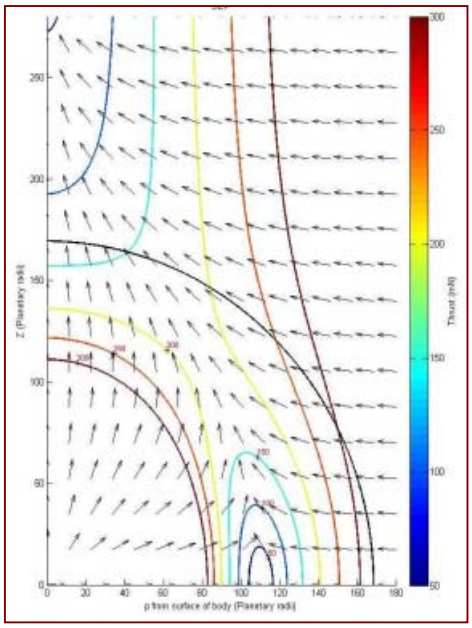

Figure 12. Mars two-body type III orbits (from McKay et al., 2011)

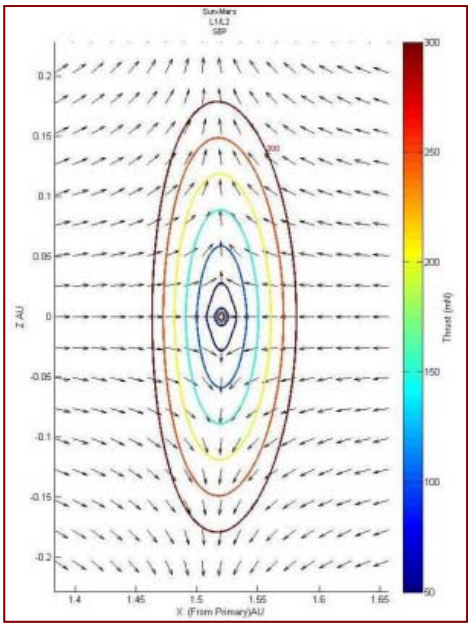

Figure 13. 3-body system equithrust contours projected onto a plane perpendicular to the ecliptic (from McKay et al., 2011)

D. LAGRANGE POINTS

Lagrangian points are defined as one of five points in the plane of revolution of two bodies in orbit around their common center of gravity at which a third body of negligible mass can remain in equilibrium with respect to the other two bodies ("Lagrangian Point," 2009). For planets within the solar system, the Sun's mass is highly dominant, which allows the resulting structure (of a planet moon) to be treated as a rotating two-body problem framed around the Sun as a fixed object. Alternately, a planet and the Sun can form the basic two-body problem within which a satellite can be stationed.

Eighteenth century mathematicians Leonhard Euler and Joseph-Louis Lagrange (for whom the points are named) discovered there are five points within this reference

where an object of negligible mass with respect to the system (such as a satellite) will remain effectively stationary (rotating with the system) as acting forces upon it are in equilibrium depicted graphically in Figures 14 and 15 ("Lagrange Points," 2014).

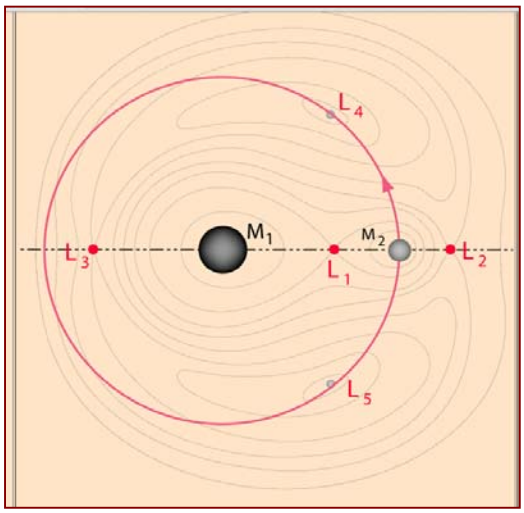

Figure 14. Gravitational equilibrium (from "Lagrange Points," 2014).

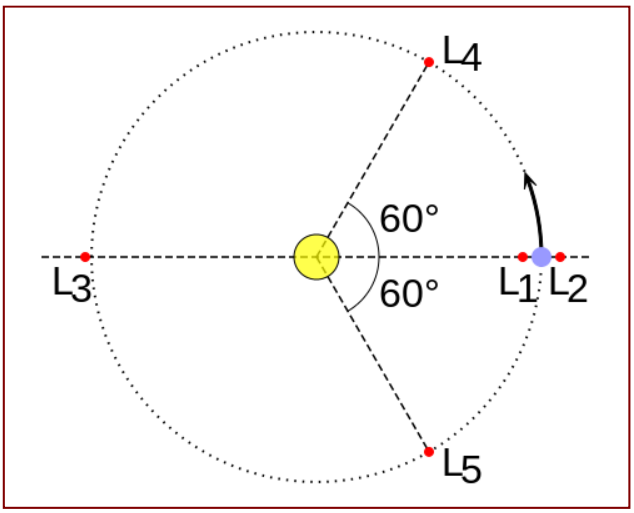

Figure 15. Angular displacement (from "List of Objects," n.d.).

As shown in Figure 14, L4 and L5 are dynamically stable (small disturbances in the orbit will dampen and eventually dissipate) while L1, L2, and L3 are not, and are therefore difficult to maintain. L1, L2, and L3 occupy positions collinear with the main bodies of the system, and therefore, are called collinear Lagrange points. L4 and L5 form an equilateral triangle between the two system bodies and are often called the triangular Lagrange points. However, as they are gravitationally stable, and therefore, an efficient location for satellite station keeping, they are also attractive to solar system debris and orbiting bodies. Within the Sun-Mars system triangular Lagrange points are occupied by Mars Trojans (asteroids named for the heroes of the Greek-Trojan war) 1999 UJ_7 (L4) and 5261 Eureka 1998 VF_{31}, 2007 NS_2, and 2001 DH_{47} (L5), as well as two additional unconfirmed asteroids 2001 FG_{24} and 2001 FR_{127} (L5) ("List of Martian," 2013).

III. EARTH-SUN-MARS GEOMETRY AND POTENTIAL ORBITS FOR MARS EARTH COMMUNICATIONS

A. EARTH MARS SUN GEOMETRY

As shown in Chapter II, the position and nature of the Sun within the Earth-Sun-Mars system creates periods where communication to the Martian surface or spacecraft in Martian orbit is impossible. This situation is acceptable for robotic missions but would present a much greater than acceptable risk to human exploration. Non-Keplerian orbits present a possible solution.

Aphelion is defined as the orbit of a planet, asteroid, or comet at which it is furthest from the Sun ("Aphelion," 2014). At aphelion, Earth is 152,098,233 km from the Sun. Mars is 249,232,432 km at aphelion. Therefore, the farthest possible distance between the planets is 401,330,665 km, with the Sun occupying an occulting position. In this worst-case scenario, communications are not only degraded by the distance but also completely blocked by the Sun. In order to enable communications, relays must be established. However, Keplerian orbital mechanics require a large number of relay satellites to provide continuous communications. Non-Keplerian orbits can extend the range of viable relay positions, and ultimately, significantly improve capability and reduce the number of satellites necessary by providing stable relays outside of the occult region.

The preliminary design for the Mars Lasercom Terminal (MLT), a proposed laser communications system for deployment to Mars orbit, includes an operating limit of within 2° of the Sun at conjunction (Scozzafava et al., 2005) (a configuration in which two celestial bodies have their least apparent separation ("Conjunction," 2014). Assuming a more conservative disk of solar interference of 21,000,000 km, Mars-Earth-Sun occultation and conjunction appear, respectively as in Figures 16 and 17.

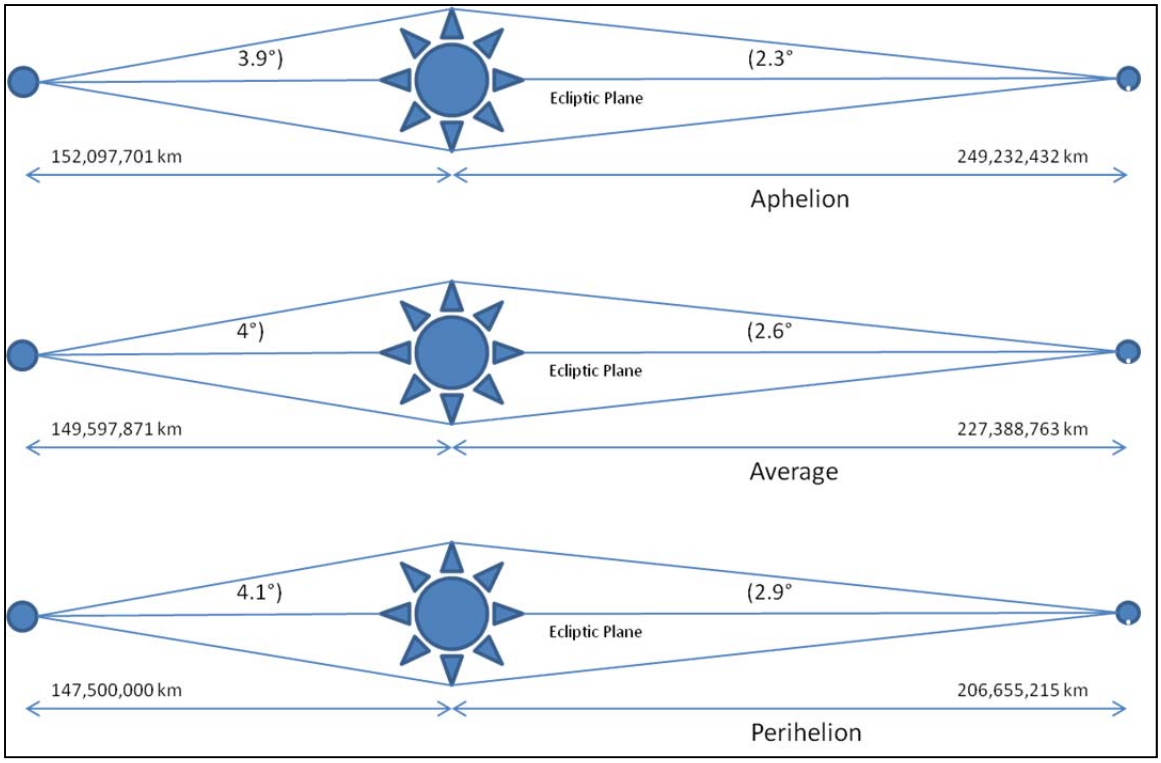

Figure 16. Solar occultation angles

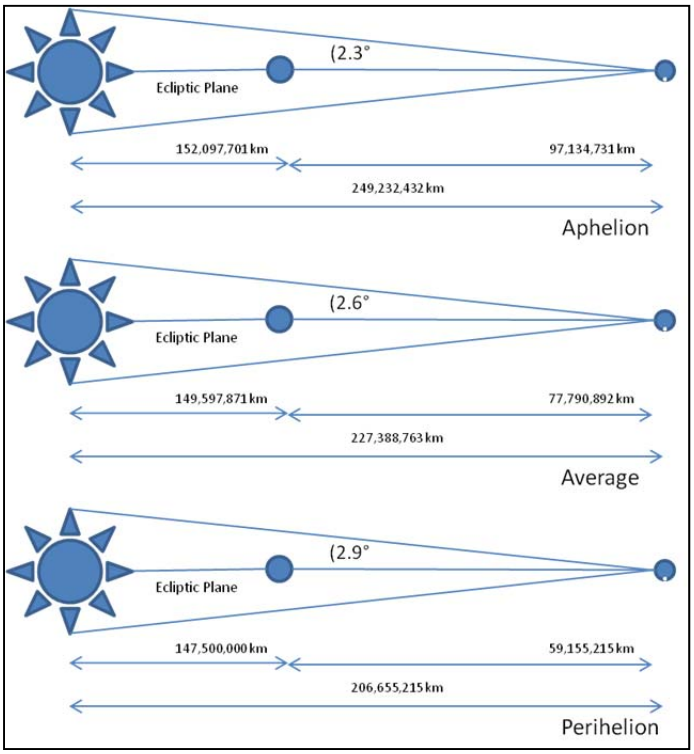

Figure 17. Solar conjunction angles

The increased radial distance of the orbiting bodies (Earth-Mars) along the ecliptic geometrically decreases the occultation angle, which consequently requires less separation between the Non-Keplerian orbiting satellite and the ecliptic plane. The minimum altitude required due to geometry is roughly 5,460,000 km, which equates to .03 AU (astronomical unit = the average distance from Earth to the Sun). This is well below the maximum threshold of McInnis non-Keplerian orbits. Due to the high transmit power requirements already in place, the detriment caused by increased altitude to Mar-Mars orbit communications is significantly less than the Mars-Earth relay benefits (additional x-band communications capability). Therefore, applying McInnis orbits as a minimum altitude presents a conservative solution to the celestial geometry, and the first of four potential orbits surveyed in this paper.

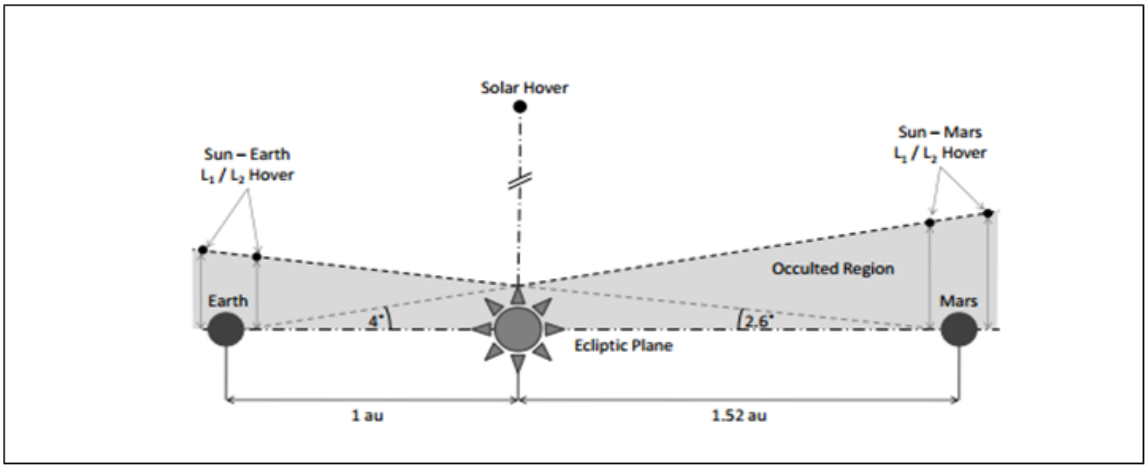

Figure 18. Mars-Earth communications relay architecture options out of the ecliptic plane (from McKay et al., 2009)

1. Orbit 1 Non-Keplerian Hover

In their paper, "Survey of Highly Non-Keplerian Orbits with Low Thrust-Propulsion," McKay et al. (2011) described the possible orbits of a 1,000 kg communication relay equipped with 300 mN continuous thrust to provide uninterrupted communication capabilities for a manned Mars mission. McKay et al. (2011) illustrated such a satellite could maintain station approximately 0.176 AU above or below the geographic poles of Mars, and consequently significantly exceed the K-band exclusion

zone of 1.5° (McKay, Macdonald, Biggs, & McInnes, 2011). Using a type II orbit as described in Chapter II and pictured above in Figure 18. they mapped an "average" occultation scenario. By super-imposing a worst case (aphelion) situation onto the occultation diagram, maximum distances and minimum expected S/N can be calculated.

By using the resulting slant range of 402,192,868 vice the previously discussed notional aphelion range of 401,330,124 km the resulting S/Ns are: best case (high power large dish uplink) S/N is 171.35 dB, and worst case (medium dish low power downlink) S/N is 0.0222 dB, which yield channel capacities of 3.715 Gbps, and 15.842 Mbps, and Eb/N0s of 23.06 dB and 0.701 dB or an overall performance decrease of 0.39%, a negligible difference to the notional/optimal link.

In contrast, the occultation period of Mars in the Earth-Sun-Mars system is approximately 780 days, while the sidereal period of Mars is approximately 687 days, which equals a 93 day period of occultation every 2.13 (Earth years) or a 12% by time outage of communications (McKay, Macdonald, Bosquillon de Frescheville, Vasile, McInnes, & Biggs, 2009). The use of Non-Keplerian type II orbits provides continuous communications (a 12% increase) in exchange for a less than ½% loss of S/N.

2. Orbit 2 Strizzi et al. L1

In their paper, "Sun-Mars Libration Points and Mars Mission Simulations," Jon D. Strizzi, Joshua M. Kutrieb, Paul E. Damphousse, and John P. Carrico (2001), examined a 2-satellite communications relay with oppositely orbiting satellites around Mars L1 and L2 first introduced by Pernicka, Henry, and Chan (1992). Carrico, Strizzi, Kutrieb, and Damphousse (2001) later assessed the utility of L1 and L2 satellites to provide communications for Mars and a Mars-Earth relay capable of bypassing the Earth-Sun-Mars occultation.

Strizzi et al. (2001) and Carrico et al. (2001) seem to have assumed the communications zone blocked by the Sun as equal to the physical area of the Sun; however, a more realistic area, which prohibits communications, is nearly 10 times as large (X-band) due to plasma effects and the high noise temperature of the Sun.

Consequently, the orbits described by Strizzi et al. (2001) are ultimately too small to provide effective communications.

Despite this apparent error, their work can be expanded as their ΔV estimates of near 2 m/s annually for a smaller orbit represent a minimal thrust estimate for the much larger (and therefore communications viable) L1/L2 halo orbit. Figure 19 shows the potential Strizzi et al. (2001) orbital geometry.

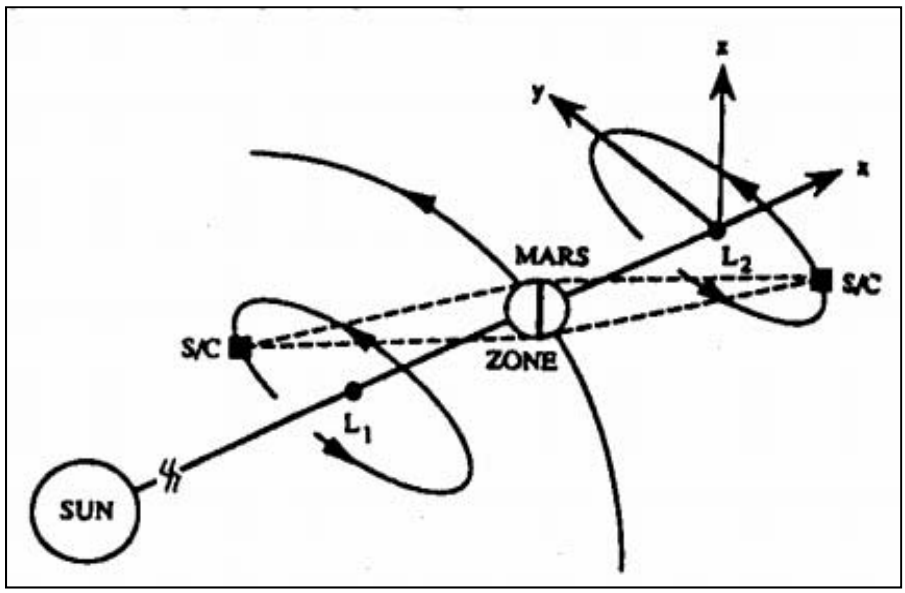

Figure 19. Sun-Mars L1 and L2 Lagrange orbits (from Strizzi et al., 2001)

Utilizing the collinear Langrange point L1 has an additional benefit of providing early warning for solar coronal mass ejections (CME); however, the Strizzi orbit also exposes the satellites to the solar exclusion zone, which ultimately requires a minimum of two satellites directly opposite each other in the same orbit, or in L1 and L2 orbits.

Within a L1 or L2 system, the first satellite (leading) will enter and exit the occlusion zone before the second satellite (lagging) enters it. Cross-linking will provide the necessary continuous communications, and in the case of a L1/L2 relay, enable nearly 99.8% of the planet to be seen continuously. Strizzi et al. (2001) expect a gap of only 1.5 minutes near the poles. However, in the event of a failure, at worst case the L1/L2 satellites could face a near 42-day long solar exclusion.

Alternately, due to their inherent stability, relay satellites could be placed at the Earth or Mars triangular Lagrange points. However, as Strizzi et al. (2001) noted, the distance of these points to either planets' surface is significant (equal to the semi-major axis of the second body, in this case Mars), which at can exceed the distance between Earth-Mars, ultimately requiring extremely large transceivers making the orbit unfeasible despite its benefit to propulsion.

3. Orbit 3 Gangale MarsSat

Gangale (2005) described a fourth possibility, and the third group of orbits surveyed by this paper, using a series of MarsSat relay satellites inclined off the ecliptic in order to lead/lag Mars and provide stable communications for at least 15 years. However, the MarsSat system requires multiple launches and multiple satellites within one or more of four candidate orbits (A, B, C, and D) shown in Figures 20 and 21.

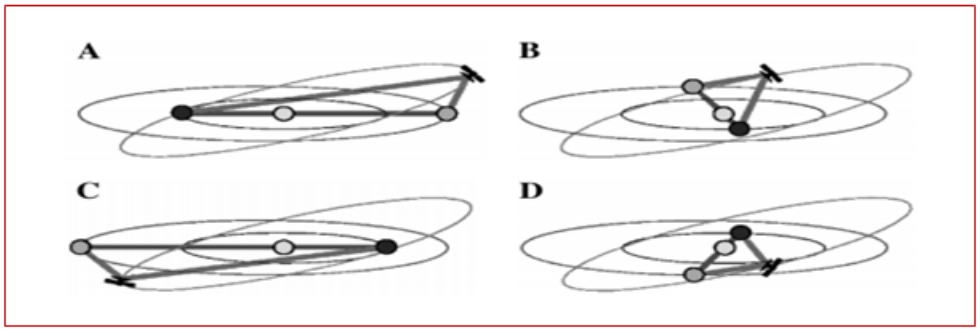

Figure 20. MarsSat candidate orbits (from Gangale, 2005)

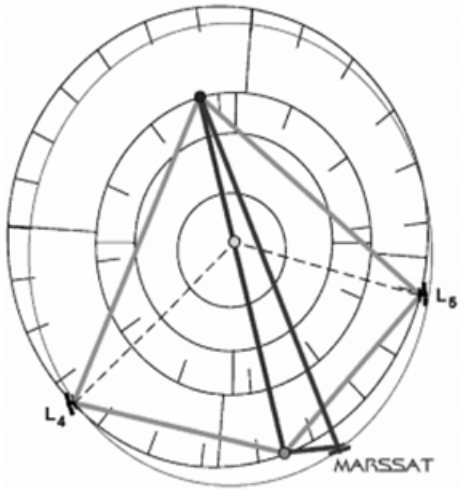

FIGURE 12. MarsSat versus Lagrange point relays.

Figure 21. L4/L5 (from Gangale, 2005)

S/N ratios for the candidate orbits vary based on their inclination, but on average (2.5° inclination) the distance between a MarsSat and Mars is 22 million km or approximately 1/10th the distance of a L4/L5 link, which if conditions are assumed equal, results in a 100 times greater signal than the Lagrangian system. If the inclination is doubled to ensure communications during the Earth-Sun-Mars occlusion, the resulting MarsSat system is still five times nearer the planet than a L4/L5 system equaling a 25:1 link budget savings over a triangular Lagrange system.

4. Orbit 4 Modified L1 Hover

As determined by Malcom Macdonald, Robert J. McKay, Massimiliano Vasile, Frcois Bosquillon de Fresheville, James Biggs, and Colin McInnes (2011), in their paper, "Low-Thrust Enabled Highly non-Keplerian Orbits in Support of Future Mars Exploration," the final system to provide continuous communications is an amalgamation of the previously described orbits. Displacement in the Y axis (of the system as described in Chapter II) requires significantly less thrust than along the Z axis. Therefore, by displacing a satellite the necessary distance to circumvent occultation along the Y is

significantly more efficient than displacing it perpendicular to the ecliptic (vertically along the Z axis) shown in Figure 22.

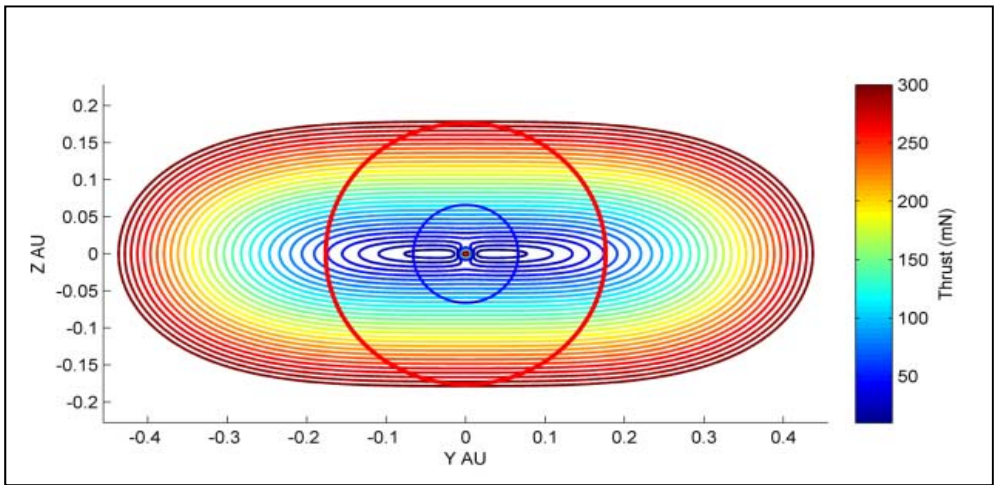

Figure 22. Equithrust contours of 1000 kg spacecraft around Mars (from Macdonald et al., 2011).

Figure 23 shows the MacDonald et al.'s (2011) equithrust contours of a 1,000 kg spacecraft in non-Keplerian orbit around Mars. The red and blue circles depict the occult region for X and Ka-bands respectively. A 45° displacement, as shown below, reduces the required thrust of a single satellite from 300 mN to 200 mN. The orbit allows for a single satellite if placed at its maximum displacement but with the potential fuel savings two satellites (L1 and L2 or opposite L1) could be used to provide coverage for a greater percentage of the surface. In the event of a failure, communication could be maintained utilizing only the remaining satellite with no risk of occlusion blocked communications.

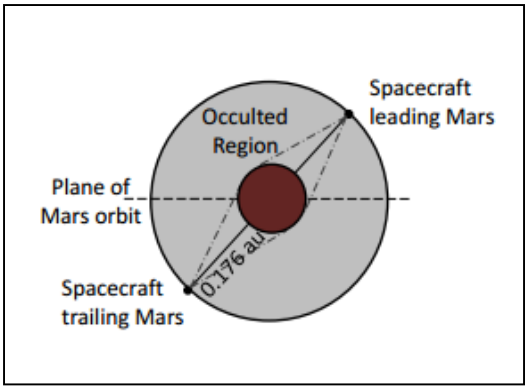

Figure 23. Alternative Architecture Along the Orbital Plane (from Macdonald et al., 2011)

THIS PAGE INTENTIONALLY LEFT BLANK

IV. ORBITAL COMPARISONS AND CONCLUSIONS

A. PROPULSION REQUIREMENTS AND ORBIT BENEFITS

Based on the two-body system resulting from the Sun-Earth-Mars geometry, Strizzi et al. (2001) analyzed L1 and L2 orbits at near Mars distances (1,000,000 kilometers ahead of and behind Mars collinearly on the ecliptic plane). Due to the large (greater than 402,000,000 kilometers) distance of communications at the ecliptic, the resulting signal to noise ratio is well within 1% of a halo orbit above or below the planet (displaced from the ecliptic plane).

The ΔV required for orbit insertion is negligibly different. Additionally, the non-Keplerian hover, Strizzi et al. (2001), and modified L1 hover, could all potentially use the Aldrin Cycler to reach mars (Chen, McConaghy, Landau, Longuski, & Aldrin, 2005; McConaghy, Longuski, & Byrnes, 2002). However, the energy required to maintain collinear Lagrange and Mars Halo orbits is markedly different. Strizzi et al. (2001) determined the annual ΔV required to maintain L1/L2 orbit as near or less than 2.45 m/s. By using Newton's second law and applying a 1,000 kg mass to Strizzi et al.'s (2001) conclusions it is possible to compare McKay et al.'s (2011) 300 mN statite to averaged thrust for a L1/ L2 satellite shown below. Strizzi et al. described orbit is decidedly less than the 300 mN thruster described by McKay et al (2011). However, McKay et al. (2011) also indicated thrust would only be required during solar occlusion, which reduces the required ΔV by a factor of 93/780 (12%). Despite this reduction, a L1/L2 orbit, in terms of propulsion, is far more efficient. When the transfer ΔV is applied, to the halo orbit the difference is increased.

$$\Delta V = a\Delta t = \frac{F}{m}(\Delta t)$$

$$2.45\ \frac{m}{s} = \frac{F}{1000\ kg}(3.156E7\ s)$$

$$F = 76.7\mu N = 0.007\ mN$$

$$\Delta V\ \frac{m}{s} = \frac{300E-3\ N}{1000\ kg}(3.156E7\ s) * \frac{93}{780}$$

$$\Delta V = 1128\ m/s$$

Therefore, for this comparison, the Strizzi L1/L2 orbit ΔV requirements are near optimal for a single satellite at an estimated 2.45 m/s, but in order to provide this fuel savings, the L1/ L2 orbit enters the occlusion zone, and therefore requires a minimum of two satellites, while a Halo orbit can provide communications with a single satellite and significantly higher propellant requirements.

Leading or lagging the planet, as recommended by Gangale's MarsSat, has a two-fold drawback of restricting communications and therefore exploration around the scientifically relevant polar region (where surface ice is visible (Carr, 1996, p. 197), and as mentioned previously, this orbit is also vulnerable to occlusion. Therefore, similar to the Strizzi et al. (2001) L1/L2 orbits, MarsSat requires a minimum of two satellites.

To counteract these drawbacks, and the significant propulsive requirements of a modified L1 hover, solar electric propulsion (SEP), orbit displacement along the Y axis, and orbit displacement about L1 can be used to reduce thrust requirements, provide limited early warning for CMEs or solar proton events, and make it possible to transition to relevant artificial equilibrium points (AEP) further reducing thrust requirements.

As outlined by Braig and McInnes (2008), Baig and McInness, (2009), and M. Ceriotti and C. R. McInnes (2010) the addition of a solar sail can drastically reduce propellant requirements for non-Keplerian orbits, including a modified L1 hover, as well as significantly expanding potential non-Keplerian orbits (asymmetrically favoring dayside L1 over nightside L2). Ultimately, a SEP enabled statite or satellite in an L1 hover is viably propulsive as compared to Strizzi et al.'s (2012) L1 orbit, which will consequently make their data capabilities more important.

B. RESULTING SIGNAL CAPABILITIES COMPARISON

As the Mars orbit to Earth signals of each of these potential satellite systems are closely aligned their function as a Mars relay becomes more important. Signal strength

and data rates of L1 L2 orbits were analyzed by W. Kok-Fai Tai (1998) and M. Danehy (1997) using generic noise temperature at multiple frequencies. Using the recommended Ka-band uplink and downlink frequencies as described in Chapter I, and more realistic noise temperatures from (Ho et al., 2002), the resulting worst case S/Ns and channel capacities for a 100W output of a satellite to 50W output ground station, similar to current field operated radios, using a non-Keplerian hover, Strizzi L1 orbit, Gangale MarsSat system, and modified Macdonald et al. displaced L1 with transition to AEP are shown in Table 5.

Table 5. Mars candidate orbit comparative S/N

Link	Orbit	S/N (dB)	Channel Capacity (Gbps)
Uplink (34450 MHZ)	Non-Keplerian Hover	63.73	10.58
Downlink (32050 MHz)		64.13	10.65
Uplink (34450 MHZ)	Strizzi L1	38.41	6.38
Downlink (32050 MHz)		34.77	5.77
Uplink (34450 MHZ)	Gangale 2.5° MarsSat	5.29	1.06
Downlink (32050 MHz)		5.69	1.12
Uplink (34450 MHZ)	Gangale 5° MarsSat	4.45	0.96
Downlink (32050 MHz)		4.86	1.01
Uplink (34450 MHZ)	Modified L1 Hover	38.41	6.38
Downlink (32050 MHz)		33.70	5.60
Uplink (34450 MHZ)	Contingency Modified L1 Hover	38.40	6.38
Downlink (32050 MHz)		33.70	5.60

As expected, the S/N is inversely proportional to distance from the planet, which makes the propulsively expensive non-Keplerian hover described by McKay et al. (2009), the most capable relay for Mars surface explorers, especially for a mission oriented towards the scientifically appealing polar regions. The channel capacity and S/N difference between the Strizzi et al. (2001) proposed L1 hover and McKay/McInnis modified L1 hover is largely negligible, in contrast to the significant difference in

propellant requirements between the orbits. However, the Strizzi orbit around L1 provides no protection against occlusion; therefore, in this case, the cost of continuous communications during occlusion is exclusively propulsive. Additionally, though the MarsSat primary and secondary orbits are beneficial in terms of fuel requirements, and viable though not ideal from a communicative standpoint, their position along Mars orbit reduces their effectiveness for other than Mars communications. Conversely, a L4/L5 satellite (not shown) provides very limited benefit for relayed Mars communications but does serve well as an interplanetary relay for missions extending much farther than Mars. Significantly, the L1 and modified L1 hover provide early warning of solar events, which is an especially important function of a manned mission's satellite relay. Due to their position (roughly 1,000,000 km) nearer the Sun than Mars, the L1 orbits provide a minimum of 5 minutes, an average of 33 minutes, and a maximum of 13 hours for a CME based on Solar and Heliospheric Observatory (SOHO)/Large Angle and Spectrometric Coronagraph (LASCO) measurements ("Coronal Mass Ejection," n.d.). This early warning could mean the difference between a successful and catastrophic mission.

C. CONCLUSION

Answers to questions asked:

1. Will 1–2 satellites be capable of maintaining continuous communication between a Mars orbit and a Mars ground mission?

Yes. As demonstrated by Strizzi et al. (2001), a L1/L2 paired hover can maintain communications for over 98% of Mars with a less than 2-minute gap in coverage. A polar statite as described by McKay et al. (2009) can more than adequately cover the polar regions without additional satellites. However, in order to provide near full planetary coverage, a minimum of two satellites is recommended.

2. Will 1–2 satellites be capable of maintaining communication between Mars and Earth, likely through the Deep Space Network

Yes. As demonstrated by extant technologies using X-band communications, Mars can be reliably contacted for the majority of its orbit. Latency tolerant programming and technologies must be used, but if combined with a Mars orbit reliable communications, are readily possible. The potential for expanded Mars-Earth

communications is significant. Additionally, there is also potential for increasing communicative ability of deep space probes or additional interplanetary missions.

3. Which frequency or frequencies will best suit Earth-Mars, and Mars relay communication?

Ka-band has emerged as a relevant and increasingly reliable avenue for communications. Its use as a primary frequency can expand data rates to Mars nearly 1,000% over previous missions. Ka-band usage is becoming increasingly common and a working proof of concept was demonstrated from Mars orbit. Additionally, its high frequency is ideal for the Martian atmosphere and could reduce orbital (and subsequent propulsion) requirements of communicating with Earth.

4. How many satellites are necessary for continuous communication, including during Mars transit through the solar occlusion zone?

By using Ka-band and non-Keplerian orbits continuous communication could be reliably provided by a single satellite/statite with sufficient offset distance from the planet. McKay et al.'s (2009) statite could provide communication from Earth to the Mars polar region throughout solar occlusion. Strizzi et al.'s (2001) concept, as well as MarsSat, could provide communication with a minimum of two satellites. The modified L1 hover could provide communication with one or two satellites during normal operations and transition to a non-Keplerian orbit outside occlusion when necessary. The modified L1 hover could also maintain function throughout occlusion despite a loss of one satellite.

5. What orbits are necessary to provide continuous communications throughout all the above mission regimes?

Each of the orbits surveyed could (albeit potentially contingent upon two or more satellites) provide communication throughout the entire mission. Propulsive requirements favor an L1 hover; however, cost (of each satellite), as well as safety (potential loss of a satellite), favor the modified L1 hover. Gangale (2005) provides the least capability at the greatest financial cost due to the multiple launches required, while Strizzi et al. (2001) provides the lowest cost but does not meet contingency operations or all flight regimes without additional satellites. Ultimately, continuous operations favor a non-Keplerian orbit provided by either a polar statite or a modified L1 hover.

D. RECOMMENDATIONS

Ultimately, due to the low loss in capacity, manageable propulsion requirements, redundancy/potential for successful contingency operations, and significant benefit provided by early warning, a pair of SEP/high ISP equipped satellites in a modified L1 hover orbit provide the greatest advantage for a manned Mars mission. If combined with artificial equilibrium points, and their requisite transit propulsion requirements, these satellites could require as little 80 mN of thrust for 12% of the year each, while providing continuous non-occluded Ka-band communication to and from Mars at a higher capacity than any other space system. Each of the orbits surveyed has potential and benefit to one or more aspects of a future mission, the advantages provided by McKay et al.'s (2011) modified L1 hover combined with a SEP/low-thrust high ISP propulsion system significantly outperform the alternatives in terms of access, capability, and availability.

APPENDIX A. NOTIONAL KEPLERIAN SIGNAL TO NOISE RATIO

Notional Keplerian

S/N

Small DSN Low Power	Noise @ Earth (dBW)	Noise @ Earth (W)	Noise @ Mars (dBW)	Noise @ Mars (W)	Total Noise (dBW)	Total Noise (W)	Signal (dBW)	Signal (W)	S/N (dB)	S/N
Earth to Mars	-119.40	1.15E-12	-118.64	1.37E-12	-118.64	1.37E-12	-115.56	2.78E-12	3.08	2.03
Mars to Earth High Power	-122.69	5.38E-13	-117.58	1.75E-12	-122.69	5.38E-13	-116.19	2.41E-12	6.50	4.47
Mars to Earth Low Power	-122.69	5.38E-13	-117.58	1.75E-12	-122.69	5.38E-13	-139.20	1.20E-14	-16.51	0.02

Large DSN Low Power	Noise @ Earth (dBW)	Noise @ Earth (W)	Noise @ Mars (dBW)	Noise @ Mars (W)	Total Noise (dBW)	Total Noise (W)	Signal (dBW)	Signal (W)	S/N (dB)	S/N
Earth to Mars	-119.40	1.15E-12	-118.64	1.37E-12	-118.64	1.37E-12	-109.29	1.18E-11	9.35	8.62
Mars to Earth High Power	-122.69	5.38E-13	-117.58	1.75E-12	-117.58	1.75E-12	-109.92	1.02E-11	7.66	5.84
Mars to Earth Low Power	-122.69	5.38E-13	-117.58	1.75E-12	-117.58	1.75E-12	-132.93	5.10E-14	-15.35	0.03

Small DSN High Power	Noise @ Earth (dBW)	Noise @ Earth (W)	Noise @ Mars (dBW)	Noise @ Mars (W)	Total Noise (dBW)	Total Noise (W)	Signal (dBW)	Signal (W)	S/N (dB)	S/N
Earth to Mars	-119.40	1.15E-12	-118.64	1.37E-12	-118.64	1.37E-12	-102.55	5.56E-11	16.09	40.67
Mars to Earth High Power	-122.69	5.38E-13	-117.58	1.75E-12	-122.69	5.38E-13	-103.18	4.81E-11	19.51	89.35
Mars to Earth Low Power	-122.69	5.38E-13	-117.58	1.75E-12	-122.69	5.38E-13	-139.20	1.20E-14	-16.51	0.02

Large DSN High Power	Noise @ Earth (dBW)	Noise @ Earth (W)	Noise @ Mars (dBW)	Noise @ Mars (W)	Total Noise (dBW)	Total Noise (W)	Signal (dBW)	Signal (W)	S/N (dB)	S/N
Earth to Mars	-119.40	1.15E-12	-118.64	1.37E-12	-118.64	1.37E-12	-96.28	2.36E-10	22.36	172.38
Mars to Earth High Power	-122.69	5.38E-13	-117.58	1.75E-12	-117.58	1.75E-12	-96.91	2.04E-10	20.67	116.76
Mars to Earth Low Power	-122.69	5.38E-13	-117.58	1.75E-12	-117.58	1.75E-12	-132.93	5.10E-14	-15.35	0.03

THIS PAGE INTENTIONALLY LEFT BLANK

APPENDIX B. NOTIONAL KEPLERIAN ORBIT CHANNEL CAPACITY

Bit Rate (Channel Capacity)

BR=B*log2(1+S/N)

Small DSN Low Power	bps	kbps	Mbps	Gbps
Earth to Mars	800459080.77	800459.08	800.46	0.80
Mars to Earth High Power	1225438705.34	1225438.71	1225.44	1.23
Mars to Earth Low Power	15935720.69	15935.72	15.94	0.02

Large DSN Low Power	bps	kbps	Mbps	Gbps
Earth to Mars	1632937930.13	1632937.93	1632.94	1.63
Mars to Earth High Power	1386803319.87	1386803.32	1386.80	1.39
Mars to Earth Low Power	20755207.37	20755.21	20.76	0.02

Small DSN High Power	bps	kbps	Mbps	Gbps
Earth to Mars	2690421169.09	2690421.17	2690.42	2.69
Mars to Earth High Power	3248723985.13	3248723.99	3248.72	3.25
Mars to Earth Low Power	3248723985.13	3248723.99	3248.72	3.25

Large DSN High Power	bps	kbps	Mbps	Gbps
Earth to Mars	3718890704.26	3718890.70	3718.89	3.72
Mars to Earth High Power	3439871590.61	3439871.59	3439.87	3.44
Mars to Earth Low Power	20755207.37	20755.21	20.76	0.02

THIS PAGE INTENTIONALLY LEFT BLANK

APPENDIX C. NOTIONAL KEPLERIAN ORBIT EB/NO AND SPECTRAL EFFICIENCY

EB/NO (S/N)*(B/data Rate) Spectral Efficiency Rb/B

Small DSN Low Power	(W/W)/(Hz/bps)	dB	bps/Hz	dB
Earth to Mars	1.27	1.04	1.60	2.04
Mars to Earth High Power	1.82	2.61	2.45	3.89
Mars to Earth Low Power	0.70	-1.54	0.03	-14.97

Large DSN Low Power				
Earth to Mars	2.64	4.21	3.27	5.14
Mars to Earth High Power	2.10	3.23	2.77	4.43
Mars to Earth Low Power	0.70	-1.53	0.04	-13.82

Small DSN High Power				
Earth to Mars	7.56	8.78	5.38	7.31
Mars to Earth High Power	13.75	11.38	6.50	8.13
Mars to Earth Low Power	0.00	-24.64	6.50	8.13

Large DSN High Power				
Earth to Mars	23.18	13.65	7.44	8.71
Mars to Earth High Power	16.97	12.30	6.88	8.38
Mars to Earth Low Power	0.70	-1.53	0.04	-13.82

THIS PAGE INTENTIONALLY LEFT BLANK

APPENDIX D. NON-KEPLERIAN HOVER SIGNAL TO NOISE RATIO

Non-Keplerian Hover

S/N

Small DSN Low Power	Noise @ Earth (dBW)	Noise @ Earth (W)	Noise @ Mars (dBW)	Noise @ Mars (W)	Total Noise (dBW)	Total Noise (W)	Signal (dBW)	Signal (W)	S/N (dB)	S/N
Earth to Mars	-119.40	1.15E-12	-118.64	1.37E-12	-118.64	1.37E-12	-115.59	2.76E-12	3.06	2.02
Mars to Earth High Power	-122.69	5.38E-13	-117.58	1.75E-12	-122.69	5.38E-13	-116.21	2.39E-12	6.47	4.44
Mars to Earth Low Power	-122.69	5.38E-13	-117.58	1.75E-12	-122.69	5.38E-13	-139.22	1.20E-14	-16.54	0.02
Large DSN Low Power	Noise @ Earth (dBW)	Noise @ Earth (W)	Noise @ Mars (dBW)	Noise @ Mars (W)	Total Noise (dBW)	Total Noise (W)	Signal (dBW)	Signal (W)	S/N (dB)	S/N
Earth to Mars	-119.40	1.15E-12	-118.64	1.37E-12	-118.64	1.37E-12	-109.31	1.17E-11	9.33	8.57
Mars to Earth High Power	-122.69	5.38E-13	-117.58	1.75E-12	-117.58	1.75E-12	-109.94	1.01E-11	7.64	5.80
Mars to Earth Low Power	-122.69	5.38E-13	-117.58	1.75E-12	-117.58	1.75E-12	-132.95	5.07E-14	-15.37	0.03
Small DSN High Power	Noise @ Earth (dBW)	Noise @ Earth (W)	Noise @ Mars (dBW)	Noise @ Mars (W)	Total Noise (dBW)	Total Noise (W)	Signal (dBW)	Signal (W)	S/N (dB)	S/N
Earth to Mars	-119.40	1.15E-12	-118.64	1.37E-12	-118.64	1.37E-12	-102.58	5.53E-11	16.07	40.43
Mars to Earth High Power	-122.69	5.38E-13	-117.58	1.75E-12	-122.69	5.38E-13	-103.20	4.78E-11	19.49	88.82
Mars to Earth Low Power	-122.69	5.38E-13	-117.58	1.75E-12	-122.69	5.38E-13	-139.22	1.20E-14	-16.54	0.02
Large DSN High Power	Noise @ Earth (dBW)	Noise @ Earth (W)	Noise @ Mars (dBW)	Noise @ Mars (W)	Total Noise (dBW)	Total Noise (W)	Signal (dBW)	Signal (W)	S/N (dB)	S/N
Earth to Mars	-119.40	1.15E-12	-118.64	1.37E-12	-118.64	1.37E-12	-96.30	2.34E-10	22.34	171.36
Mars to Earth High Power	-122.69	5.38E-13	-117.58	1.75E-12	-117.58	1.75E-12	-96.93	2.03E-10	20.65	116.07
Mars to Earth Low Power	-122.69	5.38E-13	-117.58	1.75E-12	-117.58	1.75E-12	-132.95	5.07E-14	-15.37	0.03

THIS PAGE INTENTIONALLY LEFT BLANK

APPENDIX E. NON-KEPLERIAN HOVER CHANNEL CAPACITY

Bit Rate (Channel Capacity)

BR=B*log2(1+S/N)

Small DSN Low Power	bps	kbps	Mbps	Gbps
Earth to Mars	797589341.26	797589.34	797.59	0.80
Mars to Earth High Power	1221939117.36	1221939.12	1221.94	1.22
Mars to Earth Low Power	15842361.87	15842.36	15.84	0.02

Large DSN Low Power	bps	kbps	Mbps	Gbps
Earth to Mars	1629099355.95	1629099.36	1629.10	1.63
Mars to Earth High Power	1383146316.06	1383146.32	1383.15	1.38
Mars to Earth Low Power	20634015.25	20634.02	20.63	0.02

Small DSN High Power	bps	kbps	Mbps	Gbps
Earth to Mars	2686239047.46	2686239.05	2686.24	2.69
Mars to Earth High Power	3244486289.24	3244486.29	3244.49	3.24
Mars to Earth Low Power	3244486289.24	3244486.29	3244.49	3.24

Large DSN High Power	bps	kbps	Mbps	Gbps
Earth to Mars	3714630228.39	3714630.23	3714.63	3.71
Mars to Earth High Power	3435622821.62	3435622.82	3435.62	3.44
Mars to Earth Low Power	20634015.25	20634.02	20.63	0.02

THIS PAGE INTENTIONALLY LEFT BLANK

APPENDIX F. NON-KEPLERIAN HOVER EB/NO AND SPECTRAL EFFICIENCY

EB/NO (S/N)*(B/data Rate) Spectral Efficiency Rb/B

Small DSN Low Power	(W/W)/(Hz/bps)	dB	bps/Hz	dB
Earth to Mars	1.267	1.028	1.595	2.028
Mars to Earth High Power	1.817	2.594	2.444	3.881
Mars to Earth Low Power	0.701	-1.544	0.032	-14.992

Large DSN Low Power				
Earth to Mars	2.630	4.199	3.258	5.130
Mars to Earth High Power	2.098	3.218	2.766	4.419
Mars to Earth Low Power	0.703	-1.529	0.041	-13.844

Small DSN High Power				
Earth to Mars	7.525	8.765	5.372	7.302
Mars to Earth High Power	13.688	11.363	6.489	8.122
Mars to Earth Low Power	0.003	-24.657	6.489	8.122

Large DSN High Power				
Earth to Mars	23.065	13.630	7.429	8.709
Mars to Earth High Power	16.892	12.277	6.871	8.370
Mars to Earth Low Power	0.703	-1.529	0.041	-13.844

THIS PAGE INTENTIONALLY LEFT BLANK

APPENDIX G. NON-KEPLERIAN HOVER / NOTIONAL KEPLERIAN SIGNAL TO NOISE RATIO

Non-Keplerian Hover / Notional Keplerian Comparison

S/N

Small DSN Low Power	S/N	% Lost
Earth to Mars	0.994076972	0.59
Mars to Earth High Power	0.994076972	0.59
Mars to Earth Low Power	0.994076972	0.59

Large DSN Low Power		
Earth to Mars	0.994076972	0.59
Mars to Earth High Power	0.994076972	0.59
Mars to Earth Low Power	0.994076972	0.59

Small DSN High Power		
Earth to Mars	0.994076972	0.59
Mars to Earth High Power	0.994076972	0.59
Mars to Earth Low Power	0.994076972	0.59

Large DSN High Power		
Earth to Mars	0.994076972	0.59
Mars to Earth High Power	0.994076972	0.59
Mars to Earth Low Power	0.994076972	0.59

THIS PAGE INTENTIONALLY LEFT BLANK

APPENDIX H. NON-KEPLERIAN HOVER / NOTIONAL KEPLERIAN CHANNEL CAPACITY

Bit Rate (Channel Capacity)

Small DSN Low Power	bps	% Lost
Earth to Mars	0.996414883	0.36
Mars to Earth High Power	0.997144216	0.29
Mars to Earth Low Power	0.994141538	0.59

Large DSN Low Power		
Earth to Mars	0.997649283	0.24
Mars to Earth High Power	0.997362998	0.26
Mars to Earth Low Power	0.994160881	0.58

Small DSN High Power		
Earth to Mars	0.998445551	0.16
Mars to Earth High Power	0.998695581	0.13
Mars to Earth Low Power	0.998695581	0.13

Large DSN High Power		
Earth to Mars	0.998854369	0.11
Mars to Earth High Power	0.998764847	0.12
Mars to Earth Low Power	0.994160881	0.58

THIS PAGE INTENTIONALLY LEFT BLANK

APPENDIX I. NON-KEPLERIAN HOVER / NOTIONAL KEPLERIAN EB/NO

EB/NO

Small DSN Low Power	EB/NO	% Lost
Earth to Mars	0.997653677	0.23
Mars to Earth High Power	0.996923971	0.31
Mars to Earth Low Power	0.999935053	0.01

Large DSN Low Power		
Earth to Mars	0.996419271	0.36
Mars to Earth High Power	0.996705286	0.33
Mars to Earth Low Power	0.999915598	0.01

Small DSN High Power		
Earth to Mars	0.995624619	0.44
Mars to Earth High Power	0.995375358	0.46
Mars to Earth Low Power	0.995375358	0.46

Large DSN High Power		
Earth to Mars	0.995217123	0.48
Mars to Earth High Power	0.995306328	0.47
Mars to Earth Low Power	0.999915598	0.01

THIS PAGE INTENTIONALLY LEFT BLANK

APPENDIX J. LINK BUDGET COMPARISON

Link Budget

Maximum power of DSN is 400 kW, however it is aircraft safety limited (normal use) to 20 kW)

Non-Keplerian Hover	f (GHz)	λ (m)	PTX (W)	PTX (dBW)	GTX (dB)	GRX (dB)	LFSP (dB)	LATM (dB)	PRX (dBW)
Uplink (34450 MHZ)	34.45	8.70E-03	100	20.00	80.23	64.45	-211.60	-8.00	-54.92
Downlink (32050 MHz) Low Power	32.05	9.35E-03	50	16.99	63.83	79.60	-210.97	-8.00	-58.55

Strizzi L1	f (GHz)	λ (m)	PTX (W)	PTX (dBW)	GTX (dB)	GRX (dB)	LFSP (dB)	LATM (dB)	PRX (dBW)
Uplink (34450 MHZ)	34.45	8.70E-03	100	20.00	86.50	64.45	-243.19	-8.00	-80.24
Downlink (32050 MHz) Low Power	32.05	9.35E-03	50	16.99	63.83	85.88	-242.56	-8.00	-83.87

Gangale MarsSat 2.5° Inclination	f (GHz)	λ (m)	PTX (W)	PTX (dBW)	GTX (dB)	GRX (dB)	LFSP (dB)	LATM (dB)	PRX (dBW)
Uplink (34450 MHZ)	34.45	8.70E-03	100	20.00	80.23	64.45	-270.04	-8.00	-113.36
Downlink (32050 MHz) Low Power	32.05	9.35E-03	50	16.99	63.83	79.60	-269.41	-8.00	-116.99

Gangale 5° Inclination	f (GHz)	λ (m)	PTX (W)	PTX (dBW)	GTX (dB)	GRX (dB)	LFSP (dB)	LATM (dB)	PRX (dBW)
Uplink (34450 MHZ)	34.45	8.70E-03	100	20.00	86.50	64.45	-277.14	-8.00	-114.19
Downlink (32050 MHz) Low Power	32.05	9.35E-03	50	16.99	63.83	85.88	-276.52	-8.00	-117.83

Modified L1 Hover	f (GHz)	λ (m)	PTX (W)	PTX (dBW)	GTX (dB)	GRX (dB)	LFSP (dB)	LATM (dB)	PRX (dBW)
Uplink (34450 MHZ)	34.45	8.70E-03	100	20.00	86.50	64.45	-243.19	-8.00	-80.24
Downlink (32050 MHz) Low Power	32.05	9.35E-03	50	16.99	63.83	85.88	-242.56	-8.00	-83.87

Contingency Modified L1 Hover	f (GHz)	λ (m)	PTX (W)	PTX (dBW)	GTX (dB)	GRX (dB)	LFSP (dB)	LATM (dB)	PRX (dBW)
Uplink (34450 MHZ)	34.45	8.70E-03	100	20.00	86.50	64.45	-243.19	-8.00	-80.24
Downlink (32050 MHz) Low Power	32.05	9.35E-03	50	16.99	63.83	85.88	-242.57	-8.00	-83.88

THIS PAGE INTENTIONALLY LEFT BLANK

APPENDIX K. S/N COMPARISON

S/N

Non-Keplerian Hover	Noise @ Satellite (dBW)	Noise @ Satellite (W)	Noise @ Mars (dBW)	Noise @ Mars (W)	Total Noise (dBW)	Total Noise (W)	Signal (dBW)	Signal (W)	S/N (dB)	S/N
Satellite to Mars	-122.69	5.38E-13	-118.64	1.37E-12	-118.64	1.37E-12	-54.92	3.22E-06	63.73	2.36E+06
Mars to Satellite	-122.69	5.38E-13	-118.64	1.37E-12	-122.69	5.38E-13	-58.55	1.39E-06	64.13	2.59E+06
								1.00E+00		
Strizzi L1	Noise @ Satellite (dBW)	Noise @ Satellite (W)	Noise @ Mars (dBW)	Noise @ Mars (W)	Total Noise (dBW)	Total Noise (W)	Signal (dBW)	Signal (W)	S/N (dB)	S/N
Satellite to Mars	-122.69	5.38E-13	-118.64	1.37E-12	-118.64	1.37E-12	-80.24	9.47E-09	38.41	6.93E+03
Mars to Satellite	-122.69	5.38E-13	-118.64	1.37E-12	-118.64	1.37E-12	-83.87	4.10E-09	34.77	3.00E+03

Gangale MarsSat 2.5° Inclination	Noise @ Satellite (dBW)	Noise @ Satellite (W)	Noise @ Mars (dBW)	Noise @ Mars (W)	Total Noise (dBW)	Total Noise (W)	Signal (dBW)	Signal (W)	S/N (dB)	S/N
Satellite to Mars	-119.40	1.15E-12	-118.64	1.37E-12	-118.64	1.37E-12	-113.36	4.62E-12	5.29	3.38E+00
Mars to Satellite	-122.69	5.38E-13	-118.64	1.75E-12	-122.69	5.38E-13	-116.99	2.00E-12	5.69	3.71E+00

Gangale MarsSat 5° Inclination	Noise @ Satellite (dBW)	Noise @ Satellite (W)	Noise @ Mars (dBW)	Noise @ Mars (W)	Total Noise (dBW)	Total Noise (W)	Signal (dBW)	Signal (W)	S/N (dB)	S/N
Satellite to Mars	-119.40	1.15E-12	-118.64	1.37E-12	-118.64	1.37E-12	-114.19	3.81E-12	4.45	2.79E+00
Mars to Satellite	-122.69	5.38E-13	-118.64	1.75E-12	-122.69	5.38E-13	-117.83	1.65E-12	4.86	3.06E+00
								1.00E+00		
Modified L1 Hover	Noise @ Satellite (dBW)	Noise @ Satellite (W)	Noise @ Mars (dBW)	Noise @ Mars (W)	Total Noise (dBW)	Total Noise (W)	Signal (dBW)	Signal (W)	S/N (dB)	S/N
Satellite to Mars	-119.40	1.15E-12	-118.64	1.37E-12	-118.64	1.37E-12	-80.24	9.47E-09	38.41	6.93E+03
Mars to Satellite	-122.69	5.38E-13	-118.64	1.75E-12	-117.58	1.75E-12	-83.87	4.10E-09	33.70	2.35E+03

Contingency Modified L1 Hover	Noise @ Satellite (dBW)	Noise @ Satellite (W)	Noise @ Mars (dBW)	Noise @ Mars (W)	Total Noise (dBW)	Total Noise (W)	Signal (dBW)	Signal (W)	S/N (dB)	S/N
Satellite to Mars	-119.40	1.15E-12	-118.64	1.37E-12	-118.64	1.37E-12	-80.24	9.47E-09	38.40	6.92E+03
Mars to Satellite	-122.69	5.38E-13	-118.64	1.75E-12	-117.58	1.75E-12	-83.88	4.10E-09	33.70	2.35E+03

THIS PAGE INTENTIONALLY LEFT BLANK

APPENDIX L. CHANNEL CAPACITY COMPARISON

Bit Rate (Channel Capacity)

BR=B*log2(1+S/N)

Non-Keplerian Hover	bps	kbps	Mbps	Gbps
Satellite to Mars	10584655655	10584656	10585	10.58
Mars to Satellite	10652453203	10652453	10652	10.65

Strizzi L1	bps	kbps	Mbps	Gbps
Satellite to Mars	6379388496	6379388	6379	6.38
Mars to Satellite	5775345281	5775345	5775	5.78

Gangale MarsSat 2.5° Inclination	bps	kbps	Mbps	Gbps
Satellite to Mars	1065095816	1065096	1065	1.07
Mars to Satellite	1117958522	1117959	1118	1.12

Gangale MarsSat 5° Inclination	bps	kbps	Mbps	Gbps
Satellite to Mars	960901600	960902	961	0.96
Mars to Satellite	1011415463	1011415	1011	1.01

Modified L1 Hover	bps	kbps	Mbps	Gbps
Satellite to Mars	6379282538	6379283	6379	6.38
Mars to Satellite	5598487666	5598488	5598	5.60

Contingency Modified L1 Hover		kbps	Mbps	Gbps
Satellite to Mars	6378888683	6378889	6379	6.38
Mars to Satellite	5598093922	5598094	5598	5.60

THIS PAGE INTENTIONALLY LEFT BLANK

APPENDIX M. EB/NO AND SPECTRAL EFFICIENCY

EB/NO (S/N)*(B/data Rate)

Non-Keplerian Hover	(W/W)/(Hz/bps)	dB
Satellite to Mars	111401.43	50.47
Mars to Satellite	121600.70	50.85

Strizzi L1	(W/W)/(Hz/bps)	dB
Satellite to Mars	543.13	27.35
Mars to Satellite	259.63	24.14

Gangale MarsSat 2.5° Inclination	(W/W)/(Hz/bps)	dB
Satellite to Mars	1.59	2.00
Mars to Satellite	1.66	2.20

Gangale MarsSat 5° Inclination	(W/W)/(Hz/bps)	dB
Satellite to Mars	1.45	1.62
Mars to Satellite	1.51	1.80

Modified L1 Hover	(W/W)/(Hz/bps)	dB
Satellite to Mars	543.06	27.35
Mars to Satellite	209.58	23.21

Contingency Modified L1 Hover	(W/W)/(Hz/bps)	dB
Satellite to Mars	542.80	27.35
Mars to Satellite	209.48	23.21

Spectral Efficiency Rb/B

bps/Hz	dB
21.17	13.26
21.30	13.28

bps/Hz	dB
12.76	11.06
11.55	10.63

bps/Hz	dB
2.13	3.28
2.24	3.49

bps/Hz	dB
1.92	2.84
2.02	3.06

bps/Hz	dB
12.76	11.06
11.20	10.49

bps/Hz	dB
12.76	11.06
11.20	10.49

THIS PAGE INTENTIONALLY LEFT BLANK

APPENDIX N. CME WARNING TIME

CME Warning Time

	Forward Distance (m)	Minimum Warning (s)	Average Warning (s)	Maximum Warning (s)
Non-Keplerian Hover	1000000	0.00	0.00	0.00
Strizzi L1	1000000000	309.16	1996.66	49996.66
Gangale MarsSat 2.5° Inclination	22000000000	0.00	0.00	0.00
Gangale MarsSat 5° Inclination	49846486400	0.00	0.00	0.00
Modified L1 Hover	1000000000	309.16	1996.66	49996.66
Contingency Modified L1 Hover	1000000000	309.16	1996.66	49996.66

	Forward Distance (m)	Minimum Warning (min)	Average Warning (min	Maximum Warning (min)
Non-Keplerian Hover	1000000	0.00	0.00	0.00
Strizzi L1	1000000000	5.15	33.28	833.28
Gangale MarsSat 2.5° Inclination	22000000000	0.00	0.00	0.00
Gangale MarsSat 5° Inclination	49846486400	0.00	0.00	0.00
Modified L1 Hover	1000000000	5.15	33.28	833.28
Contingency Modified L1 Hover	1000000000	5.15	33.28	833.28

THIS PAGE INTENTIONALLY LEFT BLANK

LIST OF REFERENCES

Andrews, D. J., Opgenoorth, H. J., Edberg, N. J. T., André, M., Fränz, M., Dubinin, E., Duru, F., & Witasse, O. (2013). Determination of local plasma densities with the MARSIS radar: Asymmetries in the high-altitude Martian ionosphere. *Journal of Geophysical Research: Space Physics, 118*, 1–15. Retrieved from http://www.academia.edu/6577842/Determination_of_local_plasma_densities_with_the_MARSIS_radar_Asymmetries_in_the_high-altitude_Martian_ionosphere

Aphelion. (2014). *Dictionary*. Retrieved from http://dictionary.reference.com/browse/aphelion

Atmosphere. (2014). *Merriam Webster.* Retrieved from http://www.merriam-webster.com/dictionary/atmosphere

Baig, S., & McInnes, C. R. (2008). Artificial three-body equilibria for hybrid low-thrust propulsion. *Journal of Guidance, Control, and Dynamics*, *31*(6), 1644–1655.

Baig, S., & McInnes, C. R. (2009) Artificial halo orbits for low-thrust propulsion spacecraft. *Celestial Mechanics and Dynamical Astronomy*, *104*(4), 321–335. Retrieved from http://strathprints.strath.ac.uk/8103/1/strathprints008103.pdf

Cain, F. (2009). Composition of the earth's atmosphere. Retrieved from University Today website http://www.universetoday.com/26656/composition-of-the-earths-atmosphere/

Carr, M. H. (1996). *Water on mars*. New York: Oxford University Press. Retrieved from http://www.sciencedirect.com/science/article/pii/S0019103501967946.

Carrico, J. P., Strizzi, J. D., Kutrieb, J. M., & Damphousse, P. E. (2001). Trajectory sensitivities for Sun-Mars libration point missions. Retrieved from http://www.agi.com/downloads/resources/white-papers/Trajectory-Sensitivities-for-Sun-Mar-Libration-Point-%20Missions.pdf

Chen, J. K., McConaghy, T. T., Landau, D. F., Longuski, J. M., & Aldrin, B. (2005, September–October). Powered earth-mars cycler with three-synodic-period repeat time. *Journal of Spacecraft and Rockets*, *42*(5), 921–927. Retrieved from http://buzzaldrin.com/files/pdf/2005.9-10.JOURNAL_OF_SPACECRAFT_AND_ROCKETS.PoweredEarth-MarsCyclerwithThree-Synodic-PeriodRepeatTime.pdf

Clarke suggests geosynchronous orbit. (2013). Retrieved from IEEE Global History Network http://www.ieeeghn.org/wiki/index.php/Clarke_Suggests_Geosynchronous_Orbit

Conjunction. (2014). *Merriam Webster*. Retrieved from http://www.merriam-webster.com/dictionary/conjunction

Coronal mass ejection. (n.d.). *Wikipedia*. Last modified September 12, 2014. Retrieved from: http://en.wiki|pedia.org/wiki/Coronal_mass_ejection

Danehy, M. S. (1997). *Martian communications network design trade study* (master's thesis). Retrieved from http://scholarworks.sjsu.edu/cgi/viewcontent.cgi?article=2566&context=etd_theses

Dreyer, J. L. E., & Tycho Brahe. (1890). *A picture of scientific life and work in the sixteenth century*. Edinburgh: Adam and Charles Black.

DSN telecommunications link design handbook (810-005). (n.d.). Pasadena, CA: Jet Propulsion Lab, California institute of Technology. Retrieved from http://deepspace.jpl.nasa.gov/dsndocs/810-005/

Dusek, H. M. (1996). Optimal station keeping at collinear points. *Progress in Astronautics and Aeronautics*, *17*, 37–44.

E_b/N_0. (2014). *Wikipedia.* Retrieved from http://en.wikipedia.org/wiki/Eb/N0.

Einstein's general relativity theory upheld. (1970, November). Pasadena, CA: Jet Propulsion Lab, California Institute of Technology and National Aeronautics Space Administration. Retrieved from http://www.jpl.nasa.gov/releases/70s/release_1970_0566.html

Forward, R. L. (1991). Statite: A spacecraft that does not orbit. *Journal of Spacecraft and Rockets*, *28*(5), 606–611.

Gangale, T. (2005). MarsSat: Assured communication with Mars. *Annals of the New York Academy of Sciences*, 1065, 296–310.

Hill, S. A., (n.d.). Orbital eccentricy demo. *Wikipedia.* Retrieved from http://en.wikipedia.org/wiki/Kepler_orbit#mediaviewer/File:OrbitalEccentricityDemo.svg

Ho, C. M., Sue, M. K., & Golshan, N. (2002). Martian atmospheric effects on radio wave propagation. Pasadena, CA: Jet Propulsion Lab, California Institute of Technology. Retrieved from http://trs-new.jpl.nasa.gov/dspace/bitstream/2014/12321/1/01-0365.pdf

Ho, C., Golshan, N., & Kliore, A. (2002). Radio wave propagation handbook for communication on and around mars. JPL Publication, 02(5). Retrieved from http://descanso.jpl.nasa.gov/Propagation/mars/MarsPub020318.pdfhttp://descanso.jpl.nasa.gov/Propagation/mars/MarsPub020318.pdf

Ho, C., Slobin, S., & Gritton, K. (2005). Atmospheric noise temperature induced by clouds and other weather phenomena at SHF band (1–45 GHz). JPLD-32584. Edwards Air Force Base, CA: United States Air Force. Retrieved from http://descanso.jpl.nasa.gov/Propagation/Ka_Band/JPL-D32584_1.pdf

Ho, C., Slobin, S., Sue, M., & Njoku, E. (2002, May). Mars background noise temperatures received by spacecraft antennas. IPN progress report 42-149. Retrieved from http://ipnpr.jpl.nasa.gov/progress_report/42-149/149C.pdf

ITU Radiocommunication Assembly. (2001). Recommendation ITU-R P.372-7 radio noise. Retrieved from International Telecommunication Union https://www.itu.int/dms_pubrec/itu-r/rec/p/R-REC-P.372-7-200102-S!!PDF-E.pdf

KA-band. (n.d.). Retrieved August 12, 2014, from General Dynamics SATCOM http://www.gdsatcom.com/kaband.php

Kepler, J. (1609). *Astronomia Nova.* [New Astronomy]. Retrieved from Mathmatical Association of America http://www.maa.org/publications/periodicals/convergence/johannes-keplers-astronomia-nova

Kepler, J. (1622). *Epitome Astronomiae Copernicanae [Summary of Copernican Astronomy*] (Linz ("Lentiis ad Danubium"), (Austria): Johann Planck.

Kepler, J. (1619). *Harmonices mundi [The harmony of the world]*. Linz, Austria: Johann Planck.

Lagrange points of the Earth-Moon system. (2014). Retrieved from http://hyperphysics.phy-astr.gsu.edu/hbase/mechanics/lagpt.html

Lagrangian point. (2009). *The free dictionary*. Retrieved from http://www.thefreedictionary.com/Lagrangian+point

Lemmon, T. J., & Mondragon, A. R. (2010). First-order special relativisitic corrections to Kepler's orbits. Retrieved from http://arxiv.org/pdf/1012.5438.pdf

List of Martian trojans. (2013). Last updated September 11, 2014. Retrieved from http://www.minorplanetcenter.org/iau/lists/MarsTrojans.html

List of objects at Lagrangian points. (n.d.). *Wikipedia*. Last modified August 19, 2014. Retrieved from http://en.wikipedia.org/wiki/List_of_objects_at_Lagrangian_points

Mahaffy, P. R., Webster, C. R., Atreya, S. K., Franz, H., Wong, M., Conrad, P. G. …MSL Science Team. (2013). Abundance and isotopic composition of gases in the Martian atmosphere from the curiosity rover. *Science*, *341*(6143), 263–266.

Macdonald, M., Mckay, R., Vasile, M., Bosquillon de Frescheville, F., Biggs, J., & McInnes, C. (2011). Low-thrust enabled highly non-Keplerian orbits in support of future Mars exploration. *Journal of Guidance, Control and Dynamics, 34*(5), 1396–1411.

McConaghy, T. T., Longuski, J. M., & Byrnes, D. V. (2002). Analysis of a broad class of earth-mars cycler trajectories. Retrieved from http://buzzaldrin.com/files/pdf/2002/AIAA_PAPER.Analysis_of_a_Broad_Class_of_Earth-Mars_Cycler_Trajectories.pdf

McInnes, C. R. (1998, September–October). Dynamics, stability and control of displaced non-Keplerian orbits. *Journal of Guidance, Control, and Dynamics*, *21*(5), 799–805.

McKay, R. J., Macdonald, M. Biggs, J., & McInnes, C. (2011). Survey of non-Keplerian orbits with low-thrust propulsion. *Journal of Guidance, Control and Dynamics*, *34*(3), 645–666. Retrieved from Strathprints Institutional Repository http://strathprints.strath.ac.uk/28996/1/Macdonald_M_et_al_Pure_Survey_of_highly_non_Keplerian_orbits_with_low_thrust_propulsion_Nov_2010.pdf

McKay, R., Macdonald, M., Bosquillon de Frescheville, F., Vasile, M., McInnes, C., & Biggs, J. (2009, 12–16 October). Non-Keplerian orbits using low thrust, high ISP propulsion systems. *60th International Astronautical Congress*. Retrieved from Strathprints Institutional Repository http://strathprints.strath.ac.uk/12919/1/strathprints0012919.pdf

Orbit. (2014). *Dictionary*. Retrieved from http://dictionary.reference.com/browse/orbit

Pernicka, H., Henry, D., & Chan, M. (1992). Use of halo orbits to provide a communication link between Earth and Mars. Retrieved from http://arc.aiaa.org/doi/abs/10.2514/6.1992-4585

Perrotto, T. J. (2011, May 3). NASA's gravity probe B confirms two Einstein space-time theories. Release 11-134. Retrieved from http://www.nasa.gov/home/hqnews/2011/may/HQ_11-134_Gravity_Probe_B.html

Provo, E. (2011a). Assured communications: mars and beyond. Retrieved from http://ccar.colorado.edu/asen5050/projects/projects_2011/provo_proj/

Provo, E. (2011b). Assured communications: mars and beyond. Basic occultation geometry. The area shaded in red is not visible from Earth, and thus cannot be directly contacted using existing telecommunications systems. Retrieved from http://ccar.colorado.edu/asen5050/projects/projects_2011/provo_proj/index_files/image003.jpg

Rising, D. (2013, November 11). Satellite hits Atlantic—but what about next one?, *Seattle Times*.

Saturn-bound spacecraft tests Einstein's theory. (2003, October 2). Retrieved from http://saturn.jpl.nasa.gov/news/newsreleases/newsrelease20031002/

S.A. 3.0. (n.d.). Conic sections [image]. *Wikipedia.* Last modified March 2012. Retrieved from http://en.wikipedia.org/wiki/Conic_section#mediaviewer/File:Conic_Sections.svg

SatCom Online. (2014). Antenna diameter, efficiency, gain, or frequency calculator. Retrieved from http://www.satcom.co.uk/article.asp?article=22

Scozzafava, J. J., Boroson, D. M., Bondurant, R. S., Pillsbury, A. D., Burnside, J. W., Spellmeyer, N. W.…Bold, D. R. (2005, October). Mars lasercom terminal. Retrieved IEEE Photonic Society from http://photonicssociety.org/newsletters/oct05/lasercom.html

Seahen. (n.d.). Conic section [image]. *Wikipedia.* Last modified March 2012. Retrieved from: http://en.wikipedia.org/wiki/Conic_section#mediaviewer/File:Conic_Sections.svg

Seiff, A. (1982). Post-Viking models for the structure of the summer atmosphere of Mars, The Mars reference atmosphere, A. J. Kliore (Ed.), *Advances in Space Research*, 2,2.

Shambayati, S., Morabito, D., Border, J. S., Davarian, F., Lee, D., Mendoza, R., Britcliffe, M., & Weinreb, S. (2014). Mars reconnaissance orbiter Ka-band (32 GHz) demonstration: Cruise phase operations. Retrieved from http://trs-new.jpl.nasa.gov/dspace/bitstream/2014/39654/1/06-0902.pdf

Strizzi, J. D., Kutrieb, J. M., Damphousse, P. E., & Carrico, J. P. (2012). Sun-mars libration points and Mars missions simulations. Retrieved from http://www.applieddefense.com/wp-content/uploads/2012/12/2001-Carrico-Sun-Mars_Libration_Points_And_Mars_Mission_Simulations.pdf

Taylor, J., Lee, D. K., & Shambayati, S. (2006). Mars reconnaissance orbiter telecommunications. Design and performance summary series. Retrieved from http://descanso.jpl.nasa.gov/DPSummary/MRO_092106.pdf.

The science: Orbital mechanics. (2009). Retrieved from http://earthobservatory.nasa.gov/Features/OrbitsHistory/page2.php

Tiscareno, M. S., Burns, J. A., Sremčević, M., Beurle, K., Hedman, M. M., Cooper, N. J. …Weiss, J. W. (2010). Physical characteristics and non-Keplerian orbital motion of "propeller" moons embedded in Saturn's rings. *The Astrophysical Journal Letters*, *718*(2), L92–L96. doi:10.1088/2041-8205/718/2/L92.

User: Magister mathematicae. (n.d.) *Wikipedia*. Last modified June 21, 2013. Retrieved from http://commons.wikimedia.org/wiki/User:Magister_Mathematicae

Zubair, M. Haider, Z., Khan, S. A., & Nasir, J. (2011). Atmospheric influences on satellite communications. *Prezeglad Elektrontochecniczny* [*Electrical Review*], *87*(5), 261–264. Retrieved from http://www.pe.org.pl/articles/2011/5/64.pdf

INITIAL DISTRIBUTION LIST

1. Defense Technical Information Center
   Ft. Belvoir, Virginia

2. Dudley Knox Library
   Naval Postgraduate School
   Monterey, California